Journal of Quantitative Spectroscopy & Radiative Transfer 300 (2023) 108529

Contents lists available at ScienceDirect

Journal of Quantitative Spectroscopy & Radiative Transfer

journal homepage: www.elsevier.com/locate/jqsrt

Multiplaform calculations of atomic radiative properties in Hf VI

E. Bokamba Motoumba [a], S. Enzonga Yoca [a,b], P. Quinet [c,d], P. Palmeri [c,*]

[a] Faculté des Sciences et Techniques, Université Marien Ngouabi, Brazzaville, BP 69, Congo
[b] Conseil Africain et Malgache pour l'Enseignement Supérieur – CAMES, Ouagadougou 01, 01 BP 134, Burkina Faso, Belgium
[c] Physique Atomique et Astrophysique, Université de Mons – UMONS, Mons, B 7000, Belgium
[d] IPNAS, Université de Liège, Liège, B 4000, Belgium

ARTICLE INFO

Article history:
Received 2 December 2022
Revised 9 February 2023
Accepted 9 February 2023
Available online 11 February 2023

Keywords:
Atomic structure
Transition probabilities
Oscillator strengths
Hf VI spectrum

ABSTRACT

In order to compute the Hf VI radiative rates and estimate their accuracy, a multiplaform approach has been adopted to calculate the oscillator strengths and transition probabilities for the 185 E1 transitions in Hf VI as classified in 2014 by Ryabtsev *et al.* (Phys Scr 2014;89:11502). It consisted of three independent atomic structure models; one based on the semi-empirical HFR method and two based on the *ab initio* MCDHF method. It was found that most of the Hf VI atomic states are strongly mixed with purity less than 50 %. This causes the computed rates to be highly model-sensitive with uncertainties of more than 100 % for most of the weak lines with line strength $S < 1$ a.u. For the strong E1 transitions with $S \geq 1$ a.u., their accuracies range between a few percents and ~ 40 %. Finally, we recommend our HFR rates except for the two lines at 223.172 Å and at 231.451 Å where the transition rates of Ryabtsev *et al.* should be used instead, although their uncertainties are greater than 50 %. It is due to strong cancellation effects affecting our calculation for these two transitions.

1. Introduction

Hafnium ($Z = 72$) is an element that could be employed in plasma-facing materials in Tokamaks [1,2] and is also produced in neutron-induced transmutation of tungsten ($Z = 74$) and its alloys that will compose the divertors in these fusion reactors [3]. As a consequence, their sputtering may generate ionic impurities of all possible charge states in the deuterium-tritium plasma. These impurities could contribute to radiation losses in controlled nuclear fusion devices. The radiative properties of these ions have therefore potential important applications in this field.

To our knowledge, few studies have been dedicated to the Hf VI spectrum. In 2012, Ryabtsev et al. [4] classified the Hf VI $5s^25p^64f^{13} - 5s^25p^54f^{13}6s$ transitions in spectra recorded in the ultraviolet (UV) range 145 – 350 Å using a low-inductive vacuum spark source and a grazing-incidence vacuum spectrograph. A few years later, they analysed the UV spectra recorded by two high-resolution vacuum spectrographs, one in the region 190 – 350 Å using the Institute of Spectroscopy Troisk grating spectrograph and the other in the spectral range 300 – 500 Å using the Meudon Observatory grating spectrograph [5]. They classified 185 Hf VI lines as transitions from the excited even-parity configurations $5s^25p^64f^{12}5d$, $5s^25p^64f^{12}6d$, $5s^25p^54f^{13}5d$, $5s^25p^54f^{13}6s$, $5s^25p^44f^{14}5d$, $5s^25p^44f^{14}6s$ and $5s5p^64f^{14}$ to the two low-lying odd-parity configurations $5s^25p^64f^{13}$ and $5s^25p^54f^{14}$, and found 137 even-parity fine-structure levels.

Following our previous work on erbium-like Lu IV, Hf V and Ta VI [6], a multiplatform approach has been adopted to determine the transition probabilities of electric dipole (E1) lines in Hf VI and evaluate their accuracy. It consisted of using the semi-empirical Hartree–Fock with relativistic corrections method (HFR) [7] and the *ab initio* multiconfiguration Dirac–Hartree–Fock with subsequent relativistic configuration-interaction method (MCDHF–RCI) [8].

2. Methods Used and Calculations

In order to determine the radiative parameters in Hf VI, we have performed three independent calculations. One was based on the semi-empirical HFR method [7] that relies on the availability of experimental energy levels while the other two were purely *ab initio* and were both based on the MCDHF method [8]. In the subsequent subsections, we provide the details of three atomic structure computations carried out in this work.

2.1. The Semi-Empirical HFR Method

In this method, the total multielectronic wavefunction of symmetry with parity Π, total angular quantum number J, and corresponding total magnetic quantum number M_J, $\Psi(\gamma \Pi J M_J)$, is developed on a basis of LSJ-coupled configuration state functions,

* Corresponding author.
E-mail address: patrick.palmeri@umons.ac.be (P. Palmeri).

https://doi.org/10.1016/j.jqsrt.2023.108529
0022-4073/

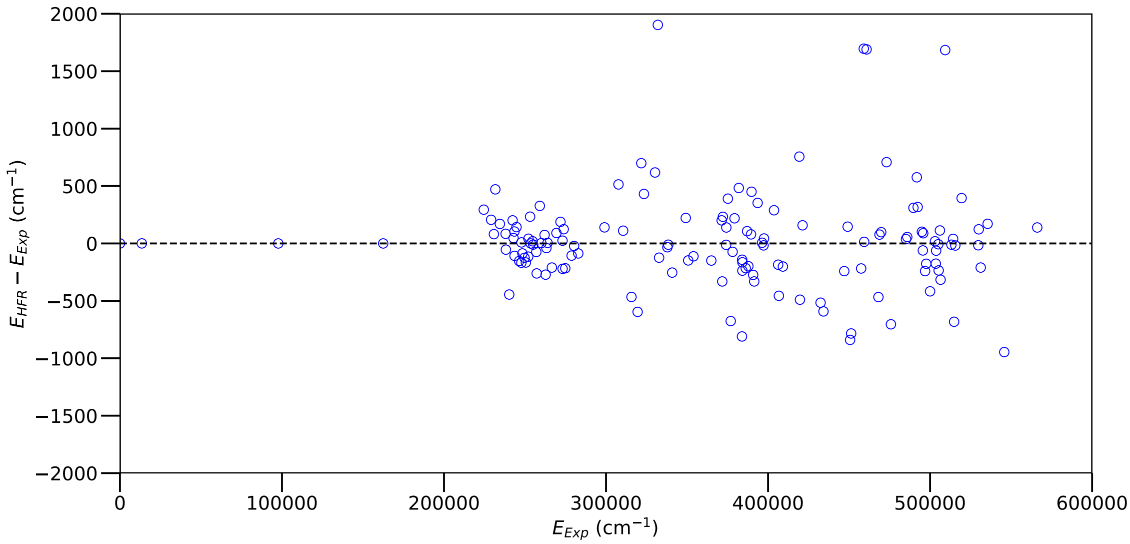

Fig. 1. Comparison of HFR energy levels with respect to experiment [5]. The energy difference is plotted versus the experimental energy. The root mean square of the differences is equal to 423 cm^{-1}. Black dashed line: straight line of equality.

$\Phi(\alpha\Pi LSJM_J)$, where L and S are respectively the total orbital and total spin quantum numbers:

$$\Psi\left(\gamma\Pi JM_J\right) = \sum_{\alpha} c_{\alpha\gamma}\,\Phi\left(\alpha\Pi LSJM_J\right) \tag{1}$$

where $c_{\alpha\gamma}$ are matrix elements of the representation where γ and α respectively refer to a particular total wavefunction and LSJ-coupled basis function.

The latter are built on Slater determinants of one-electron orbitals:

$$\phi_{n\ell m}(r,\theta,\varphi) = \frac{P_{n\ell}(r)}{r} Y_{lm}(\theta,\varphi) \tag{2}$$

where $Y_{\ell m}$ are the spherical harmonics, and $P_{n\ell}$ are the radial parts of the orbitals that are solutions of the radial integro-differential HFR equations solved separately for each multielectronic configuration considered in the expansion given by Eq. (1) [7].

In this calculation, the total wavefunctions were built by superpositions of the following electronic configurations within the framework of the configuration interaction (CI) approach: $5s^25p^64f^{13}$ + $5s^25p^64f^{12}$(6p + 7p + 5f + 6f + 7f) + $5s^25p^54f^{14}$ + $5s^25p^44f^{14}$(6p + 7p + 5f + 6f + 7f) + $5s5p^54f^{14}$(5d + 6s) in the odd parity, and $5s^25p^64f^{12}$(5d + 6d + 7d + 6s + 7s) + $5s^25p^54f^{13}$(5d + 6d + 7d + 6s + 7s) + $5s5p^64f^{14}$ + $5s5p^54f^{14}$(6p + 5f) + $5s^25p^44f^{14}$(5d + 6d + 7d + 6s + 7s) in the even parity. In order to include the effects of distant configurations, all the Slater radial integrals of the multielectronic Hamiltonian were first scaled down by 0.85 according to a well-established practice [7]. The wavefunctions were further improved by adjusting some radial parameters of the Hamiltonian, *i.e* those characterizing the interactions within and between known configurations, so as to mininize the differences between the eigenvalues and the experimental level energies of Ryabtsev *et al.* [5]. They are reported in Table 1. The average deviations between the experimental and calculated energy levels in the fitting procedure were 0 cm^{-1} for the odd parity and 430 cm^{-1} for the even parity.

2.2. The Ab Initio MCDHF Method

The present *ab initio* calculations were focused on the electric dipole transitions starting from the two odd-parity levels with symmetries $J^{\Pi} = 5/2^o, 7/2^o$ of the ground configuration, *i.e.* $5s^25p^64f^{13}$, and from the two excited odd-parity levels with symmetries $J^{\Pi} = 1/2^o, 3/2^o$ belonging to the configuration $5s^25p^54f^{14}$ and ending on the 137 even-parity levels with symmetries $J^{\Pi} = 1/2^e - 9/2^e$ belonging to the configurations $5s^25p^64f^{12}(5d,6d)$, $5s^25p^54f^{13}(5d,6s)$, $5s^25p^44f^{14}(5d,6s)$ and $5s5p^64f^{14}$ classified by Ryabtsev et al. [5]. They were based on the MCDHF method as implemented in the latest version of the GRASP package, namely GRASP2018 [8], where atomic state functions (ASF) of a symmetry with parity Π, total angular quantum J, and its corresponding total magnetic quantum number M_J, *i.e.* $\Psi(\gamma\Pi JM_J)$, are represented on a basis of configuration state functions (CSFs), $\Phi(\alpha\Pi JM_J)$,

$$\Psi\left(\gamma\Pi JM_J\right) = \sum_{\alpha} c_{\alpha\gamma}\,\Phi\left(\alpha\Pi JM_J\right) \tag{3}$$

where $c_{\alpha\gamma}$ are matrix elements of the representation, in which γ and α respectively refer to a particular ASF and CSF.

The CSFs are in turn built on *jj*-coupled *N*-electron Slater determinants of monoelectronic spin-orbitals, $\phi_{n\kappa m}(r,\theta,\varphi)$:

$$\Phi(\alpha\Pi JM_J) = \sum_{m_1\cdots m_N} \langle \kappa_1 m_1 \cdots \kappa_N m_N | (\kappa_1\cdots\kappa_N)_A; X, JM_J\rangle \times \frac{1}{\sqrt{N!}} \begin{vmatrix} \phi_{n_1\kappa_1 m_1}(r_1,\theta_1,\varphi_1) & \cdots & \phi_{n_N\kappa_N m_N}(r_1,\theta_1,\varphi_1) \\ \vdots & \ddots & \vdots \\ \phi_{n_1\kappa_1 m_1}(r_N,\theta_N,\varphi_N) & \cdots & \phi_{n_N\kappa_N m_N}(r_N,\theta_N,\varphi_N) \end{vmatrix} \tag{4}$$

where the angular coefficients $\langle \kappa_1 m_1 \cdots \kappa_N m_N | (\kappa_1\cdots\kappa_N)_A; X, JM_J\rangle$ are the generalized Clebsch-Gordan coefficients as defined in [9].

The spin-orbitals are given by:

$$\phi_{n\kappa m}(r,\theta,\varphi) = \frac{1}{r}\begin{pmatrix} P_{n\kappa}(r)\chi_{\kappa m}(\theta,\varphi) \\ iQ_{n\kappa}(r)\chi_{\kappa m}(\theta,\varphi) \end{pmatrix} \tag{5}$$

where $\chi_{\kappa m}$ are the spinor spherical harmonics, and $P_{n\kappa}$ and $Q_{n\kappa}$ are respectively the large and the small radial components that are solutions of the radial integro-differential MCDHF equations [9]. In Eq. (5), the relativistic quantum number κ is defined by:

$$\kappa = \pm\left(j + \frac{1}{2}\right) \tag{6}$$

where $\kappa = -(j + 1/2)a$, with a fixed according to:

$$\ell = j - \frac{1}{2}a;\;\; a = \pm 1 \tag{7}$$

Table 1
Radial parameters (in cm^{-1}) adopted in the HFR model.

Configuration	Parameter	*Ab initio*	Fitted	Unc.	Ratio	Remark[a]
Odd Parity						
$4f^{13}$	E_{av}	9 379	9 304	0	/	
	ζ_{4f}	3 910	3 860	0	0.99	
$5p^54f^{14}$	E_{av}	144 722	122 947	0	/	
	ζ_{5p}	44 366	43 377	0	0.98	
$5p^44f^{14}6p$	E_{av}	603 097	/	/	/	F
$5p^44f^{14}7p$	E_{av}	747 678	/	/	/	F
$5p^44f^{14}5f$	E_{av}	698 581	/	/	/	F
$5p^44f^{14}6f$	E_{av}	790 741	/	/	/	F
$5p^44f^{14}7f$	E_{av}	839 774	/	/	/	F
$5s5p^54f^{14}5d$	E_{av}	750 601	/	/	/	F
$5s5p^54f^{14}6s$	E_{av}	821 762	/	/	/	F
$4f^{12}6p$	E_{av}	398 203	/	/	/	F
$4f^{12}7p$	E_{av}	547 186	/	/	/	F
$4f^{12}5f$	E_{av}	497 446	/	/	/	F
$4f^{12}6f$	E_{av}	591 157	/	/	/	F
$4f^{12}7f$	E_{av}	641 024	/	/	/	F
Even Parity						
$4f^{12}5d$	E_{av}	242 100	253 718	136	/	
	$F^2(4f4f)$	169 487	134 724	1 175	0.80	R1
	$F^4(4f4f)$	107 320	98 429	3 222	0.92	R2
	$F^6(4f4f)$	77 495	74 509	3 299	0.96	R3
	α	/	14.5	15	/	R4
	β	/	-309	678	/	R5
	γ	/	-541	760	/	R6
	ζ_{4f}	4 084	3 936	35	0.96	R7
	ζ_{5d}	3 341	3 283	83	0.98	R8
	$F^2(4f5d)$	41 113	33 380	965	0.81	R9
	$F^4(4f5d)$	19 700	15 995	462	0.81	R9
	$G^1(4f5d)$	15 084	12 207	431	0.81	R10
	$G^3(4f5d)$	13 666	11 059	391	0.81	R10
	$G^5(4f5d)$	10 797	8 738	309	0.81	R10
$4f^{12}6d$	E_{av}	497 311	508 595	123	/	
	$F^2(4f4f)$	170 072	135 196	1 179	0.80	R1
	$F^4(4f4f)$	107 723	98 801	3 234	0.92	R2
	$F^6(4f4f)$	77 795	74 801	3 312	0.96	R3
	α	/	14.5	15	/	R4
	β	/	-309	678	/	R5
	γ	/	-541	760	/	R6
	ζ_{4f}	4 096	3 949	35	0.96	R7
	ζ_{6d}	880	865	22	0.98	R8
	$F^2(4f6d)$	10 244	8 317	240	0.81	R9
	$F^4(4f6d)$	4 465	3 626	105	0.81	R9
	$G^1(4f6d)$	3 012	2 438	86	0.81	R10
	$G^3(4f6d)$	2 999	2 444	86	0.82	R10
	$G^5(4f6d)$	2 450	1 997	70	0.82	R10
$4f^{12}7d$	E_{av}	592 905	/	/	/	F
$4f^{12}6s$	E_{av}	323 531	/	/	/	F
$4f^{12}7s$	E_{av}	514 961	/	/	/	F
$5p^54f^{13}5d$	E_{av}	335 112	335 399	139	/	
	ζ_{5p}	46 768	46 349	106	0.99	R11
	ζ_{4f}	3 926	3 810	34	0.97	R7
	ζ_{5d}	3 127	3 071	77	0.98	R8
	$F^2(4f5p)$	65 743	48 272	1 282	0.73	R12
	$F^2(4f5d)$	40 193	32 206	931	0.80	R9
	$F^4(4f5d)$	19 319	15 479	447	0.80	R9
	$F^2(5p5d)$	72 028	61 487	1 461	0.85	R13
	$G^2(4f5p)$	29 055	22 939	1 068	0.79	R14
	$G^4(4f5p)$	23 478	18 535	863	0.79	R14
	$G^1(4f5d)$	15 377	12 155	429	0.79	R10
	$G^3(4f5d)$	13 668	10 804	382	0.79	R10
	$G^5(4f5d)$	10 729	8 481	300	0.79	R10
	$G^1(5p5d)$	86 223	60 294	460	0.70	R15
	$G^3(5p5d)$	53 937	37 719	288	0.70	R15
$5p^54f^{13}6d$	E_{av}	580 255	/	/	/	F
$5p^54f^{13}7d$	E_{av}	674 301	/	/	/	F
$5p^54f^{13}6s$	E_{av}	480 664	406 406	116	/	
	ζ_{5p}	47 755	47 327	108	0.99	R11
	ζ_{4f}	3 934	3 819	34	0.97	R7
	$F^2(4f5p)$	66 454	48 795	1 295	0.73	R12
	$G^2(4f5p)$	29 289	23 122	1 076	0.79	R14
	$G^4(4f5p)$	23 728	18 732	872	0.79	R14
	$G^3(4f6s)$	4 660	4 387	1 821	0.94	
	$G^1(5p6s)$	9 597	9 004	681	0.94	R16

(*continued on next page*)

Table 1 (*continued*)

Configuration	Parameter	*Ab initio*	Fitted	Unc.	Ratio	Remark[a]
$5p^5 4f^{13} 6s$	E_{av}	408 162	/	/	/	F
$5p^5 4f^{13} 7s$	E_{av}	596 817	/	/	/	F
$5s5p^6 4f^{14}$	E_{av}	441 391	/	/	/	F
$5s5p^6 4f^{13} 6p$	E_{av}	894 190	/	/	/	F
$5s5p^6 4f^{13} 5f$	E_{av}	989 789	/	/	/	F
$5p^4 4f^{14} 5d$	E_{av}	464 345	455 999	252	/	
	$F^2(5p5p)$	89 426	71 236	1 793	0.80	R17
	ζ_{5p}	45 099	44 693	102	0.99	R11
	ζ_{5d}	2 935	2 882	72	0.98	R8
	$F^2(5p5d)$	70 482	60 166	1 429	0.85	R13
	$G^1(5p5d)$	84 039	58 764	448	0.70	R15
	$G^3(5p5d)$	52 546	36 743	280	0.70	R15
$5p^4 4f^{14} 6d$	E_{av}	700 115	/	/	/	F
$5p^4 4f^{14} 7d$	E_{av}	792 791	/	/	/	F
$5p^4 4f^{14} 6s$	E_{av}	529 824	518 642	264	/	
	$F^2(5p5p)$	90 140	71 804	1 807	0.80	R17
	ζ_{5p}	46 044	45 631	104	0.99	R11
	$G^1(5p6s)$	9 618	9 023	683	0.94	R16
$5p^4 4f^{14} 7s$	E_{av}	715 751	/	/	/	F
$4f^{12} 5d - 5p^5 4f^{13} 5d$	$R^2(5p4f, 4f4f)$	-9 453	-7 326	462	0.78	R18
	$R^4(5p4f, 4f4f)$	-2 559	-1 983	125	0.78	R18
	$R^2(5p5p, 4f5p)$	-39 662	-30 737	1 936	0.78	R18
	$R^2(5p5d, 4f5d)$	-29 360	-22 753	1 433	0.78	R18
	$R^4(5p5d, 4f5d)$	-18 828	-14 591	919	0.78	R18
	$R^1(5p5d, 5d4f)$	-26 380	-20 444	1 288	0.78	R18
	$R^3(5p5d, 5d4f)$	-19 128	-14 824	934	0.78	R18
$4f^{12} 5d - 5p^4 4f^{14} 5d$	$R^2(5p5p, 4f4f)$	29 861	29 525	890	0.99	R19
	$R^4(5p5p, 4f4f)$	23 915	23 646	676	0.99	R19
$5p^5 4f^{13} 5d - 5p^4 4f^{14} 5d$	$R^2(4f5p, 4f4f)$	-11 441	-5 614	624	0.49	R20
	$R^4(4f5p, 4f4f)$	-3 959	-1 943	216	0.49	R20
	$R^2(5p5p, 4f5p)$	-40 669	-19 957	2 220	0.49	R20
	$R^2(5p5d, 4f5d)$	-29 854	-14 650	1 629	0.49	R20
	$R^4(5p5d, 4f5d)$	-19 073	-9 360	1 041	0.49	R20
	$R^1(5p5d, 5d4f)$	-27 153	-13 325	1 482	0.49	R20
	$R^3(5p5d, 5d4f)$	-19 461	-9 550	1 062	0.49	R20

[a] Parameters marked with the same Rn (with $n = 1 - 20$) have their variation linked together by their corresponding HFR ratios keeping fixed during the fitting procedure. Those marked with F have been fixed.

where ℓ is the non-relativistic orbital quantum number.

In the expansions represented in Eq. (3), the CSFs are generated from a set of configurations called multireference (MR) that includes the targeted or spectroscopic configurations and others that strongly interact with the latter, in which electrons from the occupied (spin-)orbitals of the MR are excited to an active set of (spin-)orbitals (AS). In what follows, the AS will be denoted by a set of $n_{max}\ell$, where n_{max} refers to the maximum principal quantum number of the spin-orbital for a fixed value of the non-relativistic orbital quantum number ℓ of an excited electronic subshell.

2.2.1. MCDHF-RCI-A

In the first MCDHF-RCI calculation, the following spectroscopic configurations were considered in the MR: $5s^2 5p^6 4f^{13}$, $5s^2 5p^5 4f^{14}$ with symmetries $J^\Pi = 1/2^o - 7/2^o$; $5s^2 5p^6 4f^{12}(5d, 6d)$, $5s^2 5p^5 4f^{13}(5d, 6s)$, $5s^2 5p^4 4f^{14}(5d, 6s)$ and $5s5p^6 4f^{14}$ with symmetries $J^\Pi = 1/2^e - 9/2^e$. The AS was 6s6p6d6f. All single and double electron excitations from the occupied orbitals except the core subshells up to the 4d orbital which were kept closed were considered to build a basis of 4 126 144 CSFs. The latter has been further reduced to 3 545 069 CSFs by deleting the ones that weakly interact with the CSFs of the MR through the Dirac-Coulomnb-Breit (DCB) Hamiltonian [8]. The orbitals were obtained in separate Dirac–Hartree–Fock Extended Average Level (EAL) [8,9] self-consistent-field (SCF) optimizations on a single configuration as follows: all the core orbitals, meaning 1s to 4d, along with the 5s, 5p and 4f valence orbitals were optimized on the ground configuration $5s^2 5p^6 4f^{13}$; for the others, each $n\ell$ orbital of the AS were optimized on a configuration of the corresponding type $5s^2 5p^6 4f^{12} n\ell$. In the relativistic configuration interaction (RCI) procedure, the Dirac-Coulomb-Breit Hamiltonian with the addition of quantum electrodynamics (QED) terms such as the self-energy (SE) and vacuum polarization (VP) interactions has been diagonalized on the 3 545 069 CSFs basis in order to determine the corresponding eigenvalues and eigenvectors.

2.2.2. MCDHF-RCI-B

We have followed a different strategy in this second *ab initio* calculation. More specifically, the same MR as in our MCDHF-RCI-A calculation was retained, but the AS was here 7s6p7d5f with one correlation shell per ℓ symmetry, and a different optimization scheme was chosen. It was carried out in three steps. In the first step, the core orbitals along with the 5s, 5p and 4f orbitals were optimized on the ground configuration using an EAL procedure similar to our preceding *ab initio* calculation. The second step consisted of a MCDHF Extended Optimize Level (EOL) [8] SCF optimization of all the other spectroscopic orbitals, namely 6s, 5d and 6d, on all the 333 levels of the MR keeping the orbitals of the previous step frozen. In the last step, the CSFs basis was extended to 3 261 592 CSFs by considering all the single and double excitations from the occupied 5s, 5p, 5d, 6s, 6d and 4f orbitals to the AS and by keeping only the CSFs that interact significatively with the 333 CSFs of the MR through the DCB hamiltonian. The correlation orbitals, *i.e.* 7s, 6p, 7d and 5f, were then optimized on the 333 levels of the MR during a MCHDF EOL SCF procedure. Finally, a RCI calculation was carried out on the 3 261 592 CSFs basis where the QED interactions were added to the DCB hamiltonian.

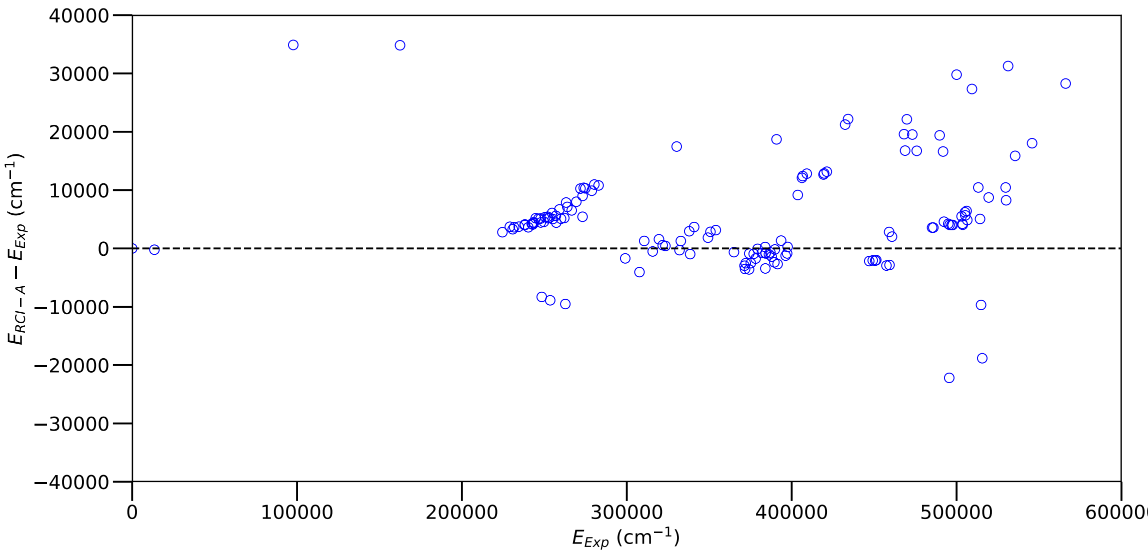

Fig. 2. Comparison of MCDHF-RCI-A energy levels with respect to experiment [5]. The energy difference is plotted versus the experimental energy. The root mean square of the differences is equal to 10 392 cm^{-1}. Black dashed line: straight line of equality.

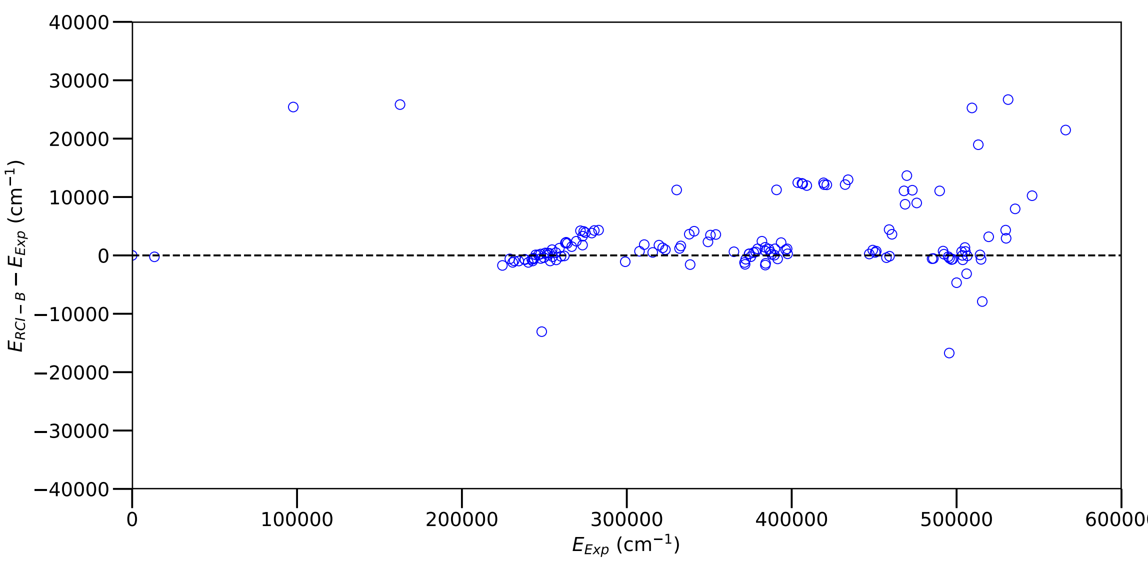

Fig. 3. Comparison of MCDHF-RCI-B energy levels with respect to experiment [5]. The energy difference is plotted versus the experimental energy. The root mean square of the differences is equal to 6 977 cm^{-1}. Black dashed line: straight line of equality.

3. Results

In Table 2, our three sets of computed level energies, namely HFR, MCDHF-RCI-A and MCDHF-RCI-B, are compared to the experimental values of Ryabtsev et al. [5]. For the purpose of conciseness as we focus on the transition rates, the many unobserved even-parity levels that are located between the observed ones are not shown. Also reported in this table are the *LS*-coupling compositions as computed in our HFR model showing the first three major components. As one can see, most of the levels are strongly mixed with a purity less or equal to 50 %. For the purpose of clarity, we have plotted in Figs. 1–3 the difference between the level energy calculated in our three independent models and the one determined experimentally by Ryabtsev et al. [5] as function of the latter. The root mean squares (RMS) of these differences were respectively: 423 cm^{-1} for our HFR model (Fig. 1); 10 392 cm^{-1} for our MCDHF-RCI-A model (Fig. 2); 6 977 cm^{-1} for our MCDHF-RCI-B model (Fig. 3). As expected, our semi-empirical HFR model reproduces the experimental energy spectrum better, as it was fitted to mininize these energy differences. Regarding our *ab initio* calculations, one can also clearly notice that our MCDHF-RCI-B level energies reproduce the experiment much better than our MCDHF-RCI-A model, probably due to a better representation of the correlation effects through a more adequate choice of orbitals, meaning the use of correlation orbitals correcting the spectroscopic ones.

The transition probabilities, *gA*, oscillator strengths in the logarithmic scale, *log gf*, with their corresponding uncertainty indicators, namely the cancellation factor (CF) as defined by Cowan [7] for the HFR method and the uncertainty indicator *dT* as defined by Ekman et al. [10] for the MCDHF method, as computed in our three independent models are reported in Table 3 for the 185 E1 transitions observed in the spectral range 193 Å $< \lambda <$ 474 Å by Ryabtsev et al. [5]. Our *ab initio gA*- and *log gf*-values, *i.e.* those computed in both our MCDHF models, have been rescaled using the experimental wavelengths [5]. The corresponding transition probabilities as calculated by Ryabtsev et al. [5] using the same HFR method but with more limited CI expansions are also presented for comparison. The latter have been used as refer-

Table 2
Comparison between the present calculated and the available experimental energy levels in Hf VI.

i	E_{exp}[a] (cm^{-1})	E_{HFR}[b] (cm^{-1})	E_{RCI-A}[c] (cm^{-1})	E_{RCI-B}[d] (cm^{-1})	J	*LS* Composition[e]
1	0	0	0	0	7/2	100% 4f^{13} ^{2}F^o
2	13513.6	13514	13292	13270	5/2	100% 4f^{13} ^{2}F^o
3	97710	97710	132600	123123	3/2	100% 5p^{5}4f^{14} ^{2}P^o
4	162465	162465	197296	188295	1/2	100% 5p^{5}4f^{14} ^{2}P^o
5	224555	224849	227338	222833	7/2	36% 4f^{12}5d (^{3}H)^{4}F + 21% 4f^{12}5d (^{3}F)^{4}F + 10% 4f^{12}5d (^{4}F)^{4}D
6	229066	229272	232783	228471	9/2	25% 4f^{12}5d (^{3}F)^{4}G + 15% 4f^{12}5d (^{3}F)^{2}G + 15% 4f^{12}5d (^{1}G)^{2}H
7	230797	230878	234091	229598	7/2	34% 4f^{12}5d (^{3}H)^{4}F + 17% 4f^{12}5d (^{3}H)^{4}G + 16% 4f^{12}5d (^{3}F)^{4}D
8	231679	232150	235312	230753	9/2	44% 4f^{12}5d (^{3}H)^{4}G + 15% 4f^{12}5d (^{3}F)^{4}F + 13% 4f^{12}5d (3H)^{4}H
9	234488	234658	238214	233524	7/2	62% 4f^{12}5d (^{3}H)^{2}F + 10% 4f^{12}5d (^{3}H)^{4}G + 8% 4f^{12}5d (^{3}F)^{4}G
10	238045	238129	242036	237383	7/2	31% 4f^{12}5d (^{3}F)^{4}D + 19% 4f^{12}5d (^{1}G)^{2}G + 8% 4f^{12}5d (^{3}H)^{4}H
11	238197	238143	242311	237462	9/2	36% 4f^{12}5d (^{3}H)^{2}G + 13% 4f^{12}5d (^{3}H)^{4}H + 12% 4f^{12}5d (^{3}F)^{2}G
12	240254	239809	243881	239052	7/2	26% 4f^{12}5d (^{3}F)^{4}G + 17% 4f^{12}5d (^{3}F)^{4}H + 15% 4f^{12}5d (^{3}H)^{4}F
13	242344	242545	246563	241664	9/2	29% 4f^{12}5d (^{3}H)^{4}I + 14% 4f^{12}5d (^{3}H)^{2}G + 13% 4f^{12}5d (^{1}G)^{2}H
14	242914	242961	247014	241958	7/2	35% 4f^{12}5d (^{3}H)^{4}G + 19% 4f^{12}5d (^{3}F)^{4}G + 12% 4f^{12}5d (^{3}F)^{4}D
15	243466	243570	247936	242979	5/2	32% 4f^{12}5d (^{3}H)^{2}F + 17% 4f^{12}5d (^{3}F)^{4}D + 15% 4f^{12}5d (^{3}H)^{4}F
16	243553	243445	247867	242947	9/2	21% 4f^{12}5d (^{3}H)^{2}H + 15 4f^{12}5d (^{3}F)^{2}G + 12% 4f^{12}5d (^{3}F)^{4}H
17	244753	244895	249937	244842	7/2	32% 4f^{12}5d (^{3}F)^{4}H + 20% 4f^{12}5d (^{3}F)^{2}F + 9% 4f^{12}5d (^{1}D)^{2}G
18	246387	246234	251482	246470	5/2	34% 4f^{12}5d (^{3}F)^{2}D + 33% 4f^{12}5d (^{3}F)^{4}F + 9% 4f^{12}5d (^{3}H)^{4}F
19	247755	247587	252878	247989	7/2	23% 4f^{12}5d (^{3}F)^{4}F + 13% 4f^{12}5d (^{3}F)^{2}F + 12% 4f^{12}5d (^{3}F)^{4}G
20	247805	247814	252257	247272	5/2	34% 4f^{12}5d (^{3}H)^{4}G + 26% 4f^{12}5d (^{3}F)^{4}P + 11% 4f^{12}5d (^{1}G)^{2}D
21	248405	248318	240093	235343	3/2	39% 4f^{12}5d (^{3}H)^{4}F + 33% 4f^{12}5d (^{3}F)^{2}P + 13% 4f^{12}5d (^{3}F)^{2}D
22	249722	249597	254275	249341	9/2	22% 4f^{12}5d (^{3}F)^{4}F + 15% 4f^{12}5d (^{3}H)^{2}H + 13% 4f^{12}5d (^{3}H)^{4}I
23	250546	250380	255927	250961	7/2	43% 4f^{12}5d (^{3}F)^{2}G + 12% 4f^{12}5d (^{1}D)^{2}F + 9% 4f^{12}5d (^{3}H)^{4}H
24	251975	251860	257405	252366	7/2	28% 4f^{12}5d (^{3}F)^{2}F + 24% 4f^{12}5d (^{3}F)^{4}F + 10% 4f^{12}5d (^{3}H)^{2}G
25	252130	252171	257316	252154	9/2	35% 4f^{12}5d (^{3}F)^{2}H + 19% 4f^{12}5d (^{3}F)^{4}G + 14% 4f^{12}5d (^{3}F)^{2}G
26	253134	253367	258393	253489	7/2	27% 4f^{12}5d (^{1}G)^{2}F + 15% 4f^{12}5d (^{3}H)^{4}H + 15% 4f^{12}5d (^{3}F)^{4}H
27	253530	253530	244641	252577	3/2	24% 4f^{12}5d (^{3}F)^{4}F + 18% 4f^{12}5d (^{3}F)^{2}D + 16% 4f^{12}5d (^{3}F)^{4}D
28	254671	254690	260754	255653	5/2	37% 4f^{12}5d (^{3}F)^{2}D + 14% 4f^{12}5d (^{3}F)^{2}F + 12 4f^{12}5d (^{3}F)^{4}G
29	255057	255047	260100	254841	9/2	24% 4f^{12}5d (^{3}H)^{4}I + 23% 4f^{12}5d (^{1}G)^{2}G + 16% 4f^{12}5d (^{1}G)^{2}H
30	256978	256904	262561	257450	7/2	25% 4f^{12}5d (^{3}H)^{2}G + 20% 4f^{12}5d (^{1}G)^{2}G + 12% 4f^{12}5d (^{1}G)^{2}F
31	257206	256945	261628	256436	5/2	43% 4f^{12}5d (^{1}G)^{2}D + 24% 4f^{12}5d (^{3}H)^{2}F + 9% 4f^{12}5d (^{3}H)^{4}F
32	259130	259457	265822	260365	5/2	15% 4f^{12}5d (^{3}P)^{4}D + 14% 4f^{12}5d (^{1}G)^{2}F + 12% 4f^{12}5d (^{3}F)^{2}D
33	260097	260100	265186	259937	7/2	21% 4f^{12}5d (^{3}H)^{4}H + 15% 4f^{12}5d (^{1}G)^{2}F + 13% 4f^{12}5d (^{1}D)^{2}G
34	262079	262153	267297	261985	9/2	19% 4f^{12}5d (^{1}I)^{2}G + 18% 4f^{12}5d (^{1}G)^{2}G + 16% 4f^{12}5d (^{3}H)^{4}H
35	262729	262457	253201	264865	3/2	37% 4f^{12}5d (^{3}F)^{2}D + 20% 4f^{12}5d (^{3}P)^{4}D + 17% 4f^{12}5d (^{1}G)^{2}D
36	263211	263171	271088	265456	7/2	23% 4f^{12}5d (^{3}P)^{4}D + 11% 4f^{12}5d (^{3}P)^{4}F + 9% 4f^{12}5d (^{3}F)^{2}G
37	263904	263909	271024	265964	5/2	28% 4f^{12}5d (^{1}G)^{2}F + 25% 4f^{12}5d (^{3}F)^{2}F + 12% 4f^{12}5d (^{3}H)^{2}F
38	266584	266374	273109	268086	9/2	66% 4f^{12}5d (^{1}I)^{2}G + 9% 4f^{12}5d (^{1}G)^{2}G + 5% 4f^{12}5d (^{1}I)^{2}H
39	269387	269478	277391	271816	5/2	25% 4f^{12}5d (^{3}P)^{4}D + 20% 4f^{12}5d (^{1}D)^{2}F + 9% 4f^{12}5d (^{3}F)^{4}D
40	271883	272071	282146	276102	3/2	37% 4f^{12}5d (^{3}P)^{4}F + 13% 4f^{12}5d (^{3}P)^{2}D + 12% 4f^{12}5d (^{3}P)^{4}P
41	273155	273179	278585	274919	7/2	78% 4f^{12}5d (^{1}I)^{2}G + 10% 4f^{12}5d (^{3}H)^{2}G + 3% 5p^{5}4f^{13}5d (^{3}D)^{2}G
42	273199	272978	282203	276490	5/2	22% 4f^{12}5d (^{1}D)^{2}D + 22% 4f^{12}5d (^{3}P)^{2}D + 21% 4f^{12}5d (^{3}P)^{4}D
43	273871	273995	284266	277975	3/2	39% 4f^{12}5d (^{3}P)^{4}F + 21% 4f^{12}5d (^{3}P)^{4}P + 12% 4f^{12}5d (^{3}P)^{4}D
44	274853	274637	285160	278750	5/2	45% 4f^{12}5d (^{3}P)^{4}F + 18% 4f^{12}5d (^{3}P)^{2}F + 16% 4f^{12}5d (^{1}D)^{2}D
45	278751	278645	288645	282577	5/2	43% 4f^{12}5d (^{3}P)^{2}D + 18% 4f^{12}5d (^{3}P)^{4}F + 11% 4f^{12}5d (^{1}D)^{2}F
46	280302	280280	291262	284569	3/2	30% 4f^{12}5d (^{3}P)^{2}P + 23% 4f^{12}5d (^{3}P)^{4}P + 18% 4f^{12}5d (^{1}D)^{2}P
47	282873	282786	293677	287196	3/2	40% 4f^{12}5d (^{3}P)^{2}D + 24% 4f^{12}5d (^{3}P)^{2}P + 8% 4f^{12}5d (^{3}P)^{4}P
48	299053	299193	297349	297967	9/2	25% 5p^{5}4f^{13}5d (^{1}F)^{2}H + 19% 5p^{5}4f^{13}5d (^{3}F)^{4}F + 10% 5p^{5}4f^{13}5d (^{1}F)^{2}G
49	307683	308197	303626	308385	7/2	24% 5p^{5}4f^{13}5d (^{3}G)^{2}F + 18% 5p^{5}4f^{14}5d (^{1}D)^{2}G + 16% 5p^{5}4f^{13}5d (^{3}F)^{4}H
50	310567	310678	311852	312414	5/2	34% 5p^{5}4f^{13}5d (^{1}D)^{2}F + 11% 5p^{5}4f^{13}5d (^{3}D)^{4}F + 9% 5p^{5}4f^{13}5d (^{1}D)^{2}D
51	315701	315235	315184	316209	7/2	28% 5p^{5}4f^{13}5d (^{1}G)^{2}F + 16% 5p^{5}4f^{13}5d (^{3}G)^{2}F + 15% 5p^{5}4f^{13}5d (^{3}G)^{4}F
52	319492	318896	321069	321244	7/2	40% 4f^{12}6s (^{3}F)^{4}F + 19% 4f^{12}6s (^{3}F)^{2}F + 12% 5p^{5}4f^{13}5d (^{1}D)^{2}F
53	321759	322458	322322	323055	5/2	14% 5p^{5}4f^{13}5d (^{1}G)^{2}F + 11% 4f^{12}6s (^{3}F)^{2}F + 9% 5p^{5}4f^{13}5d (^{3}F)^{2}D
54	323415	323846	323840	324384	7/2	22% 5p^{5}4f^{13}5d (^{1}G)^{2}G + 14% 5p^{5}4f^{13}5d (^{3}D)^{2}G + 10% 5p^{5}4f^{13}5d (^{3}F)^{4}H
55	330247	330865	347717	341457	5/2	22% 5p^{5}4f^{13}5d (^{3}D)^{2}F + 17% 5p^{5}4f^{13}5d (^{3}D)^{4}D + 15% 5p^{5}4f^{13}5d (^{3}D)^{4}F
56	331970	333873	331677	333162	5/2	45% 4f^{12}5d (^{1}S)^{2}D + 9% 5p^{5}4f^{13}5d (^{3}G)^{2}D + 6% 5p^{5}4f^{13}5d (^{3}F)^{4}P
57	332759	332635	334034	334378	9/2	17% 5p^{5}4f^{13}5d (^{1}G)^{2}G + 15% 5p^{5}4f^{13}5d (^{3}G)^{2}H + 11% 5p^{5}4f^{13}5d (^{3}G)^{4}G
58	337874	337841	340823	341507	9/2	23% 5p^{5}4f^{13}5d (^{1}G)^{2}H + 21% 5p^{5}4f^{13}5d (^{3}D)^{4}G + 10% 5p^{5}4f^{13}5d (^{3}G)^{4}G
59	338413	338402	337441	336837	5/2	41% 4f^{12}5d (^{1}S)^{2}D + 12% 5p^{5}4f^{13}5d (^{3}G)^{2}D + 8% 5p^{5}4f^{13}5d (^{3}F)^{4}P
60	340838	340584	344509	344974	7/2	15% 5p^{5}4f^{13}5d (^{3}D)^{4}F + 11% 5p^{5}4f^{13}5d (^{3}G)^{4}G + 9% 5p^{5}4f^{13}5d (^{3}D)^{4}G
61	349222	349444	351066	351538	3/2	18% 5p^{5}4f^{13}5d (^{3}G)^{4}F + 15% 4f^{12}6s (^{3}P)^{4}P + 14% 5p^{5}4f^{13}5d (^{3}G)^{4}D
62	350718	350570	353563	354192	7/2	24% 5p^{5}4f^{13}5d (^{3}G)^{4}H + 14% 5p^{5}4f^{13}5d (^{1}G)^{2}G + 12% 5p^{5}4f^{13}5d (^{3}F)^{4}H
63	353977	353865	357120	357554	5/2	29% 5p54f^{13}5d (^{3}G)^{4}G + 11% 5p^{5}4f^{13}5d (^{1}G)^{2}F + 10% 5p^{5}4f^{13}5d (^{3}D)^{2}F
64	364979	364830	364347	365601	5/2	22% 5p^{5}4f^{13}5d (^{3}D)^{4}D + 19% 5p^{5}4f^{13}5d (^{3}D)^{4}P + 8% 5p^{5}4f^{13}5d (^{1}G)^{2}D
65	371386	371587	368420	370166	7/2	32% 5p^{5}4f^{13}6s (^{1}F)^{2}F + 23% 5p^{5}4f^{13}6s (^{3}F)^{4}F + 18% 5p^{5}4f^{13}6s (^{3}D)^{4}D
66	371732	371401	368207	370197	9/2	59% 5p^{5}4f^{13}6s (^{3}F)^{4}F + 11% 5p^{5}4f^{13}6s (^{3}G)^{4}G + 7% 5p^{5}4f^{13}5d (^{3}G)^{4}I
67	372126	372358	369598	371467	5/2	45% 5p^{5}4f^{13}6s (^{1}F)^{2}F + 14% 5p^{5}4f^{13}6s (^{3}D)^{2}D + 9% 5p^{5}4f^{13}6s (^{3}D)^{4}D
68	374123	374111	370529	374364	9/2	43% 5p^{5}4f^{13}5d (^{3}G)^{4}I + 19% 5p^{5}4f^{13}5d (^{1}F)^{2}H + 8% 5p^{5}4f^{13}5d (^{3}G)^{2}H
69	374257	374396	373378	374535	3/2	28% 5p^{5}4f^{13}5d (^{1}G)^{2}D + 22% 5p^{5}4f^{13}5d (^{3}G)^{4}D + 22% 5p^{5}4f^{13}5d (^{3}F)^{2}P
70	375213	375603	372690	374986	7/2	41% 5p^{5}4f^{13}6s (^{3}F)^{2}F + 24% 5p^{5}4f^{13}6s (^{1}F)^{2}F + 11% 5p^{5}4f^{13}6s (^{3}G)^{4}G
71	376952	376276	376028	377441	5/2	26% 5p^{5}4f^{13}5d (^{1}G)^{2}F + 12% 5p^{5}4f^{13}5d (^{3}G)^{2}F + 12% 5p^{5}4f^{13}6s (^{1}F)^{2}F
72	378129	378056	376385	378715	9/2	69% 5p^{5}4f^{13}6s (^{3}G)^{2}G + 21% 5p^{5}4f^{13}6s (^{3}G)^{4}G + 6% 5p^{5}4f^{13}6s (^{3}F)^{4}F
73	379318	379537	379248	380439	7/2	20% 5p^{5}4f^{13}5d (^{3}D)^{4}D + 17% 5p^{5}4f^{13}5d (^{3}D)^{2}F + 11% 5p^{5}4f^{13}5d (^{3}F)^{4}D

(*continued on next page*)

Table 2 (*continued*)

i	E_{exp} [a] (cm^{-1})	E_{HFR} [b] (cm^{-1})	E_{RCI-A} [c] (cm^{-1})	E_{RCI-B} [d] (cm^{-1})	J	*LS* Composition [e]
74	381941	382424	381155	384366	5/2	20% $5p^54f^{13}5d\ (^3G)^2F$ + 16% $5p^54f^{13}5d\ (^1D)^2F$ + 9% $5p^54f^{13}5d\ (^3F)^4G$
75	383918	383108	384165	385299	7/2	23% $5p^54f^{13}5d\ (^3G)^2G$ + 11% $5p^54f^{13}5d\ (^3D)^2F$ + 11% $5p^54f^{13}6s\ (^3F)^4F$
76	384016	383874	380586	382358	7/2	25% $5p^54f^{13}6s\ (^3F)^4F$ + 15% $5p^54f^{13}6s\ (^3F)^2F$ + 12% $5p^54f^{13}5d\ (^3G)^4H$
77	384138	383901	383288	384871	3/2	44% $5p^54f^{13}6s\ (^1D)^2D$ + 12% $5p^54f^{13}6s\ (^3F)^4F$ + 12% $5p^54f^{13}6s\ (^3D)^4D$
78	384190	384026	383419	382831	5/2	45% $5p^54f^{13}6s\ (^3F)^4F$ + 9% $5p^54f^{13}6s\ (^3G)^4G$ + 8% $5p^54f^{13}5d\ (^3G)^4G$
79	386218	386003	385211	387297	5/2	49% $5p^54f^{13}6s\ (^1D)^2D$ + 28% $5p^54f^{13}6s\ (^3D)^4D$ + 8% $5p^54f^{13}6s\ (^3F)^2F$
80	387070	387177	386380	387624	9/2	21% $5p^54f^{13}5d\ (^1D)^2G$ + 17% $5p^54f^{13}5d\ (^3G)^4H$ + 15% $5p^54f^{13}5d\ (^3G)^2H$
81	387844	387646	386447	388013	5/2	26% $5p^54f^{13}5d\ (^3G)^4G$ + 21% $5p^54f^{13}5d\ (^3G)^4F$ + 8% $5p^54f^{13}5d\ (^3G)^2F$
82	389487	389566	387103	389530	3/2	34% $5p^54f^{13}6s\ (^3F)^4F$ + 14% $5p^54f^{13}6s\ (^3D)^4D$ + 12% $5p^54f^{13}5d\ (^3F)^2D$
83	389800	390250	389626	390924	7/2	26% $5p^54f^{13}5d\ (^3G)^4G$ + 21% $5p^54f^{13}5d\ (^3G)^4H$ + 19% $5p^54f^{13}5d\ (^3G)^2G$
84	390811	390537	409515	402034	5/2	28% $5p^44f^{14}5d\ (^3P)^4d$ + 26% $5p^54f^{13}6s\ (^3F)^2F$ + 7% $5p^54f^{13}6s\ (^3D)^4D$
85	391459	391128	388775	390857	5/2	27% $5p^44f^{14}5d\ (^3P)^4d$ + 19% $5p^54f^{13}6s\ (^3F)^2F$ + 18% $5p^54f^{13}6s\ (^3D)^4D$
86	393577	393930	394920	395765	9/2	36% $5p^54f^{13}6s\ (^1G)^2G$ + 30% $5p^54f^{13}6s\ (^3G)^4G$ + 13% $5p^54f^{13}6s\ (^3G)^2G$
87	396329	396335	395094	397287	7/2	45% $5p^54f^{13}6s\ (^1G)^2G$ + 30% $5p^54f^{13}6s\ (^3G)^4G$ + 22% $5p^54f^{13}6s\ (^3G)^2G$
88	397227	397210	396371	398350	3/2	63% $5p^54f^{13}6s\ (^3D)^2D$ + 32% $5p^54f^{13}6s\ (^3D)^4D$ + 3% $5p^54f^{13}6s\ (^3F)^4F$
89	397520	397563	397780	397791	7/2	30% $5p^54f^{13}5d\ (^1D)^2F$ + 10% $5p^54f^{13}5d\ (^3F)^2G$ + 7% $5p^44f^{14}5d\ (^3P)^4F$
90	403691	403980	412855	416153	7/2	46% $5p^44f^{14}5d\ (^3P)^2F$ + 24% $5p^44f^{14}5d\ (^1D)^2G$ + 9% $5p^44f^{14}5d\ (^3P)^4D$
91	406238	406053	418349	418572	9/2	29% $5p^54f^{13}5d\ (^3D)^2G$ + 18% $5p^54f^{13}5d\ (^3F)^2G$ + 11% $5p^54f^{13}5d\ (^3G)^2G$
92	406678	406222	419083	418928	5/2	32% $5p^54f^{13}5d\ (^3G)^2D$ + 21% $5p^54f^{13}5d\ (^1G)^2D$ + 13% $5p^54f^{13}5d\ (^3F)^2D$
93	409150	408949	421968	421114	7/2	19% $5p^54f^{13}5d\ (^3G)^2F$ + 16% $5p^54f^{13}5d\ (^3F)^2F$ + 14% $5p^54f^{13}5d\ (^1G)^2F$
94	419313	420069	431991	431742	3/2	57% $5p^54f^{13}5d\ (^3G)^2D$ + 8% $5p^54f^{13}5d\ (^1F)^2D$ + 5% $5p^54f^{13}5d\ (^3G)^4F$
95	419694	419204	432560	431815	7/2	20% $5p^54f^{13}5d\ (^1D)^2G$ + 16% $5p^54f^{13}5d\ (^3D)^2G$ + 16% $5p^54f^{13}5d\ (^3G)^2G$
96	421300	421458	434453	433387	5/2	28% $5p^54f^{13}5d\ (^3G)^2F$ + 15% $5p^54f^{13}5d\ (^3F)^2F$ + 13% $5p^54f^{13}5d\ (^1D)^2F$
97	432418	431902	453650	444549	3/2	34% $5p^44f^{14}5d\ (^3P)^4F$ + 14% $5p^44f^{14}5d\ (^3P)^2P$ + 13% $5p^44f^{14}5d\ (^1S)^2D$
98	434200	433608	456382	447162	5/2	45% $5p^44f^{14}5d\ (^3P)^4F$ + 17% $5p^44f^{14}5d\ (^1S)^2D$ + 13% $5p^44f^{14}5d\ (^1D)^2F$
99	447031	446790	444864	447269	7/2	56% $5p^54f^{13}6s\ (^3D)^4D$ + 22% $5p^54f^{13}6s\ (^3F)^4F$ + 10% $5p^54f^{13}6s\ (^1F)^2F$
100	449146	449292	447095	450050	5/2	50% $5p^54f^{13}6s\ (^3D)^2D$ + 14% $5p^54f^{13}6s\ (^3F)^4F$ + 14% $5p^54f^{13}6s\ (^3D)^4D$
101	450652	449812	448559	451165	7/2	38% $5p^54f^{13}6s\ (^1G)^2G$ + 21% $5p^54f^{13}6s\ (^3F)^2F$ + 19% $5p^54f^{13}6s\ (^3G)^4G$
102	451286	450502	449286	452008	9/2	45% $5p^54f^{13}6s\ (^1G)^2G$ + 25% $5p^54f^{13}6s\ (^3G)^4G$ + 18% $5p^54f^{13}6s\ (^3F)^4F$
103	457469	457251	454533	457081	5/2	72% $5p^54f^{13}6s\ (^3G)^4G$ + 17% $5p^54f^{13}6s\ (^1F)^2F$ + 5% $5p^54f^{13}6s\ (^3F)^4F$
104	459085	460781	461910	463502	5/2	23% $5p^44f^{14}6s\ (^3P)^4P$ + 22% $5p^54f^{13}6s\ (^1D)^2D$ + 17% $5p^54f^{13}6s\ (^3F)^2F$
105	459331	459345	456491	459191	7/2	50% $5p^54f^{13}6s\ (^3G)^2G$ + 28% $5p^54f^{13}6s\ (^3G)^4G$ + 15% $5p^54f^{13}6s\ (^1F)^2F$
106	460814	462504	462835	464427	3/2	31% $5p^54f^{13}6s\ (^1D)^2D$ + 27% $5p^54f^{13}6s\ (^3F)^4F$ + 13% $5p^54f^{13}6s\ (^3D)^2D$
107	468123	467656	487714	479175	5/2	29% $5p^44f^{14}5d\ (^3P)^4F$ + 19% $5p^44f^{14}5d\ (^3P)^2D$ + 17% $5p^44f^{14}5d\ (^1D)^2F$
108	468781	468858	485554	477539	5/2	46% $5p^44f^{14}6s\ (^3P)^4P$ + 16% $5p^54f^{13}6s\ (^1D)^2D$ + 9% $5p^44f^{14}5d\ (^3P)^2F$
109	469845	469943	491987	483513	7/2	61% $5p^44f^{14}5d\ (^1D)^2G$ + 20% $5p^44f^{14}5d\ (^3P)^2F$ + 9% $5p^44f^{14}5d\ (^1D)^2F$
110	473165	473873	492693	484327	5/2	46% $5p^44f^{14}5d\ (^3P)^2F$ + 22% $5p^44f^{14}5d\ (^3P)^4P$ + 12% $5p^44f^{14}5d\ (^1D)^2F$
111	475834	475130	492571	484815	3/2	47% $5p^44f^{14}6s\ (^3P)^2P$ + 15% $5p^44f^{14}6s\ (^1D)^2D$ + 14% $5p^44f^{14}6s\ (^3P)^4P$
112	485146	485184	488716	484583	7/2	52% $4f^{12}6d\ (^3H)^2F$ + 34% $4f^{12}6d\ (^3H)^4F$ + 5% $4f^{12}6d\ (^3H)^4G$
113	485920	485976	489493	485383	9/2	53% $4f^{12}6d\ (^3H)^2G$ + 22% $4f^{12}6d\ (^3H)^4G$ + 12% $4f^{12}6d\ (^3H)^4F$
114	489733	490043	509124	500777	1/2	49% $5p^44f^{14}6s\ (^1S)^2S$ + 37% $5p^44f^{14}6s\ (^3P)^4P$ + 12% $5p^44f^{14}6s\ (^3P)^2P$
115	491814	492390	508432	492548	5/2	23% $4f^{12}6d\ (^3F)^2D$ + 21% $4f^{12}6d\ (^3F)^4P$ + 20% $4f^{12}6d\ (^1G)^2F$
116	492346	492663	496930	492551	7/2	27% $4f^{12}6d\ (^3F)^4D$ + 20% $4f^{12}6d\ (^3F)^2F$ + 14% $4f^{12}6d\ (^3H)^4G$
117	494964	495066	499183	494739	7/2	37% $4f^{12}6d\ (^3H)^4F$ + 35% $4f^{12}6d\ (^3H)^2F$ + 10% $4f^{12}6d\ (^3H)^4G$
118	495551	495490	473361	478824	3/2	40% $5p^44f^{14}5d\ (^1D)^2P$ + 25% $5p^44f^{14}5d\ (^3P)^2P$ + 15% $5p^44f^{14}5d\ (^3P)^4F$
119	495766	495855	499808	495271	9/2	37% $4f^{12}6d\ (^3H)^2G$ + 29% $4f^{12}6d\ (^3H)^4H$ + 24% $4f^{12}6d\ (^3H)^4G$
120	496936	496695	500949	496226	5/2	60% $4f^{12}6d\ (^3H)^4F$ + 21% $4f^{12}6d\ (^3H)^2F$ + 14% $4f^{12}6d\ (^3H)^4G$
121	497613	497436	501637	496960	7/2	36% $4f^{12}6d\ (^3H)^4G$ + 22% $4f^{12}6d\ (^3H)^2G$ + 20% $4f^{12}6d\ (^3H)^4F$
122	500007	499590	529801	495330	5/2	45% $5p^44f^{14}5d\ (^3P)^2D$ + 20% $5p^44f^{14}5d\ (^1D)^2F$ + 17% $5p^44f^{14}5d\ (^1D)^2D$
123	503041	503060	508545	503679	7/2	42% $4f^{12}6d\ (^3F)^4G$ + 22% $4f^{12}6d\ (^3F)^2F$ + 6% $4f^{12}6d\ (^3H)^2G$
124	503556	503380	507787	503556	5/2	28% $4f^{12}6d\ (^3H)^4G$ + 22% $4f^{12}6d\ (^3F)^4P$ + 11% $4f^{12}6d\ (^3H)^4F$
125	503742	503679	507801	502986	7/2	21% $4f^{12}6d\ (^3F)^2G$ + 15% $4f^{12}6d\ (^3H)^4H$ + 15% $4f^{12}6d\ (^3F)^4H$
126	505071	505064	511264	506419	7/2	32% $4f^{12}6d\ (^3F)^2G$ + 17% $4f^{12}6d\ (^1D)^2F$ + 15% $4f^{12}6d\ (^3F)^4H$
127	505303	505068	510972	505982	5/2	47% $4f^{12}6d\ (^3F)^4D$ + 12% $4f^{12}6d\ (^3F)^2D$ + 10% $4f^{12}6d\ (^3F)^4P$
128	506081	506194	512503	502942	5/2	52% $4f^{12}6d\ (^3F)^2F$ + 14% $4f^{12}6d\ (^1D)^2D$ + 12% $4f^{12}6d\ (^3F)^4G$
129	506479	506163	511344	506398	3/2	53% $4f^{12}6d\ (^3F)^2D$ + 20% $4f^{12}6d\ (^3F)^4F$ + 9% $4f^{12}6d\ (^1D)^2P$
130	509331	511015	536668	534589	1/2	36% $5p44f^{14}5d\ (^1D)^2P$ + 22% $5p^44f^{14}5d\ (^3P)^2P$ + 16% $5p^44f^{14}5d\ (^1D)^2S$
131	513175	513164	523629	532131	3/2	46% $5p^44f^{14}5d\ (^1D)^2D$ + 26% $5p^44f^{14}5d\ (^3P)^2D$ + 7% $5p^44f^{14}5d\ (^3P)^4F$
132	514227	514267	519282	514309	7/2	31% $4f^{12}6d\ (^1G)^2F$ + 24% $4f^{12}6d\ (^3H)^2G$ + 19% $4f^{12}6d\ (^1G)^2G$
133	514840	514158	505150	514160	5/2	50% $4f^{12}6d\ (^1G)^2D$ + 26% $4f^{12}6d\ (^3H)^2F$ + 15% $4f^{12}6d\ (^3H)^4F$
134	515580	515562	496756	507677	5/2	53% $4f^{12}6d\ (^1G)^2F$ + 27% $4f^{12}6d\ (^3H)^4G$ + 8% $4f^{12}6d\ (^3F)^2D$
135	519474	519869	528209	522661	5/2	24% $4f^{12}6d\ (^1D)^2F$ + 22% $4f^{12}6d\ (^3P)^4D$ + 12% $4f^{12}6d\ (^3F)^4G$
136	529766	529750	540221	534091	3/2	44% $4f^{12}6d\ (^3P)^4F$ + 24% $4f^{12}6d\ (^3P)^4D$ + 10% $4f^{12}6d\ (^3P)^2P$
137	530043	530166	538303	532971	7/2	97% $4f^{12}6d\ (^1I)^2G$ + 1% $4f^{12}6d\ (^3H)^2G$ + 1% $4f^{12}6d\ (^3H)^2F$
138	531254	531044	562526	557941	1/2	33% $5p^44f^{14}5d\ (^1D)^2S$ + 18% $5p^44f^{14}5d\ (^3P)^2P$ + 16% $5s5p^64f^{14}\ (^1S)^2S$
139	535527	535698	551400	543498	1/2	45% $5p^44f^{14}6s\ (^3P)^2P$ + 19% $5p^44f^{14}6s\ (^3P)^4P$ + 14% $4f^{12}6d\ (^3P)^4P$
140	545795	544849	563835	556021	5/2	71% $5p^44f^{14}6s\ (^1D)^2D$ + 19% $5p^44f^{14}6s\ (^3P)^4P$ + 2% $5p^44f^{14}5d\ (^1S)^2D$
141	566157	566296	594432	587629	3/2	37% $5p^44f^{14}5d\ (^1S)^2D$ + 27% $5p^44f^{14}5d\ (^3P)^2D$ + 13% $5p^44f^{14}5d\ (^3P)^2P$

[a] Experimental values from Ryabtsev et al. [5];
[b] Our HFR calculation;
[c] Our MCDHF-RCI-A calculation, the transition rates are given in the Babushkin gauge;
[d] Our MCDHF-RCI-B calculation, the transition rates are given in the Babushkin gauge;
[e] Our HFR calculation. At most, only the first three major components are given.

Table 3
Comparison between the present calculated and the literature transition rates in Hf VI.

			HFR[c]				RCI-A[d]				RCI-B[e]				RYA[f]
λ[a] (Å)	i[b]	k[b]	*gA* (s^{-1})	*log gf*	*CF*[g]	*Unc.*[h]	*gA*[i] (s^{-1})	*log gf*[i]	*dT*[j]	*Unc.*[h]	*gA*[i] (s^{-1})	*log gf*[i]	*dT*[j]	*Unc.*[h]	*gA* (s^{-1})
193.600	2	137	4.12E+10	-0.64	0.34	E	3.07E+10	-0.76	0.06	E	5.04E+10	-0.55	0.03	E	4.96E+10
197.644	2	135	9.39E+09	-1.26	0.19	E	7.34E+09	-1.37	0.06	E	1.22E+10	-1.15	0.09	E	1.39E+10
197.901	1	127	6.60E+09	-1.41	0.16	E	2.46E+09	-1.84	0.09	E	2.70E+09	-1.80	0.12	E	8.80E+09
197.992	1	126	1.55E+10	-1.04	0.27	E	1.32E+10	-1.11	0.03	E	2.28E+10	-0.87	0.08	E	2.55E+10
198.520	1	125	8.77E+09	-1.29	0.30	E	1.16E+09	-2.16	0.07	E	1.50E+09	-2.05	0.07	E	1.49E+10
198.791	1	123	2.32E+10	-0.86	0.27	E	1.91E+10	-0.95	0.08	E	2.31E+10	-0.86	0.12	E	2.34E+10
199.177	2	134	3.27E+10	-0.71	0.33	E	1.84E+08	-2.96	0.01	E	1.18E+10	-1.15	0.08	E	4.49E+10
199.471	2	133	1.69E+10	-1.00	0.30	E	4.99E+09	-1.53	0.09	E	1.76E+10	-0.98	0.09	E	1.76E+10
199.715	2	132	2.60E+10	-0.81	0.28	E	2.29E+10	-0.86	0.07	E	3.30E+10	-0.70	0.07	E	3.26E+10
201.235	1	120	1.76E+09	-1.97	0.21	E	1.66E+09	-2.00	0.03	E	2.82E+09	-1.77	0.10	E	2.00E+09
201.708	1	119	2.79E+10	-0.77	0.32	E	2.56E+10	-0.81	0.08	E	3.80E+10	-0.63	0.07	E	3.58E+10
202.035	1	117	4.19E+10	-0.59	0.32	E	4.20E+10	-0.59	0.05	E	5.97E+10	-0.44	0.09	E	5.36E+10
202.854	2	129	1.24E+10	-1.12	0.29	E	8.45E+08	-2.28	0.01	E	1.29E+09	-2.10	0.11	E	1.49E+10
203.018	2	128	1.42E+10	-1.06	0.16	E	9.04E+09	-1.25	0.04	E	5.02E+09	-1.51	0.09	E	1.74E+10
203.109	1	116	1.61E+10	-1.00	0.21	E	8.13E+09	-1.30	0.02	E	5.59E+09	-1.46	0.10	E	1.69E+10
203.330	1	115	1.40E+10	-1.06	0.25	E	1.30E+09	-2.09	0.01	E	1.61E+10	-1.00	0.12	E	1.64E+10
203.981	2	125	7.20E+09	-1.35	0.17	E	1.01E+10	-1.20	0.05	E	1.51E+10	-1.03	0.07	E	1.01E+10
204.064	2	124	1.08E+10	-1.17	0.26	E	3.77E+09	-1.63	0.01	E	1.09E+10	-1.17	0.10	E	1.30E+10
205.795	1	113	4.28E+10	-0.57	0.35	E	3.83E+10	-0.61	0.05	E	4.97E+10	-0.50	0.08	E	5.26E+10
206.119	1	112	2.96E+10	-0.73	0.22	E	2.67E+10	-0.77	0.04	E	3.41E+10	-0.66	0.09	E	3.50E+10
206.569	2	121	1.26E+10	-1.09	0.28	E	1.29E+10	-1.08	0.05	E	1.65E+10	-0.98	0.08	E	1.66E+10
206.857	2	120	9.13E+09	-1.23	0.21	E	8.70E+09	-1.25	0.04	E	1.07E+10	-1.16	0.09	E	1.08E+10
212.034	2	112	3.94E+09	-1.58	0.17	E	3.41E+09	-1.64	0.06	E	8.80E+09	-1.23	0.08	E	5.00E+09
213.323	1	108	3.96E+08	-2.57	0.01	E	1.05E+08	-3.14	0.01	E	3.32E+08	-2.64	0.20	E	6.00E+08
216.302	2	111	1.15E+10	-1.09	0.67	E	7.71E+08	-2.27	0.01	E	2.45E+09	-1.76	0.05	E	1.55E+10
219.139	2	109	4.48E+09	-1.49	0.15	E	8.47E+09	-1.21	0.07	E	1.18E+10	-1.07	0.01	E	1.24E+10
219.648	2	108	1.57E+10	-0.95	0.59	E	3.62E+08	-2.58	0.01	E	1.67E+09	-1.92	0.04	E	1.72E+10
221.589	1	102	1.91E+11	0.15	0.89	D+	8.51E+10	-0.20	0.02	E	8.75E+10	-0.19	0.02	E	1.97E+11
221.898	1	101	7.85E+10	-0.24	0.56	D	1.61E+10	-0.92	0.00	E	1.89E+10	-0.86	0.07	E	7.68E+10
222.645	1	100	1.19E+11	-0.06	0.75	D+	5.52E+10	-0.39	0.03	E	4.41E+10	-0.48	0.00	E	1.19E+11
223.172	3	140	5.13E+08	-2.41	0.05	E	2.55E+08	-2.72	0.94	E	3.20E+10	-0.62	0.06	E	6.13E+10
223.566	2	106	7.18E+10	-0.27	0.91	D	4.14E+10	-0.51	0.03	E	2.15E+10	-0.79	0.03	E	6.80E+10
223.698	1	99	3.00E+10	-0.65	0.82	E	8.30E+09	-1.21	0.00	E	1.07E+10	-1.10	0.08	E	3.36E+10
224.307	2	105	1.44E+11	0.04	0.80	D+	5.63E+10	-0.37	0.03	E	5.79E+10	-0.36	0.02	E	1.45E+11
224.431	2	104	4.71E+10	-0.45	0.65	E	1.47E+10	-0.95	0.01	E	1.63E+10	-0.91	0.05	E	4.69E+10
225.248	2	103	2.24E+10	-0.77	0.70	E	5.69E+09	-1.36	0.00	E	6.80E+09	-1.29	0.10	E	2.07E+10
228.763	2	101	2.87E+09	-1.65	0.01	E	4.17E+09	-1.49	0.02	E	4.78E+09	-1.43	0.11	E	4.40E+09
230.656	3	138	8.23E+10	-0.18	0.09	D+	4.84E+09	-1.41	0.08	E	3.50E+10	-0.55	0.24	E	1.07E+11
231.451	3	136	1.59E+07	-3.89	0.03	E	7.75E+08	-2.21	0.23	E	7.82E+08	-2.20	0.04	E	4.91E+10
237.360	1	96	1.37E+09	-1.94	0.00	E	1.73E+09	-1.84	0.10	E	1.02E+09	-2.07	0.07	E	9.00E+08
238.271	1	95	5.14E+09	-1.36	0.01	E	3.07E+09	-1.58	0.21	E	1.21E+09	-1.99	0.30	E	5.50E+09
240.701	3	131	1.80E+11	0.19	0.44	C	4.49E+11	0.59	0.15	E	2.43E+11	0.33	0.07	E	1.80E+11
242.940	3	130	4.30E+11	0.58	0.66	C+	3.36E+11	0.47	0.16	E	3.92E+11	0.54	0.13	D+	4.66E+11
244.411	1	93	1.88E+12	1.23	0.84	C+	1.66E+12	1.17	0.11	C	1.66E+12	1.17	0.12	C+	1.91E+12
245.223	2	96	1.42E+12	1.11	0.83	C+	1.25E+12	1.05	0.11	C	1.24E+12	1.05	0.12	C+	1.43E+12
245.898	1	92	1.46E+12	1.12	0.86	C+	1.32E+12	1.08	0.11	C	1.32E+12	1.08	0.13	C+	1.49E+12
246.161	1	91	2.33E+12	1.33	0.86	C+	2.01E+12	1.26	0.08	C	2.04E+12	1.27	0.09	C+	2.31E+12
246.194	2	95	1.87E+12	1.23	0.85	C+	1.44E+12	1.12	0.08	D+	1.61E+12	1.16	0.10	C+	1.87E+12
246.427	2	94	9.56E+11	0.94	0.85	C+	8.32E+11	0.88	0.11	D+	8.52E+11	0.89	0.13	D+	9.67E+11
247.714	4	141	6.41E+11	0.77	0.76	C+	6.13E+11	0.75	0.14	D+	3.84E+11	0.55	0.08	E	6.66E+11
248.573	3	122	1.13E+12	1.02	0.77	C+	9.47E+11	0.94	0.15	D+	2.10E+10	-0.71	0.10	E	1.20E+12
251.357	3	118	5.39E+11	0.71	0.68	C+	1.77E+09	-1.77	0.07	E	5.90E+09	-1.25	0.24	E	5.36E+11
251.559	1	89	1.94E+10	-0.74	0.06	E	5.25E+09	-1.30	0.10	E	2.81E+09	-1.57	0.18	E	2.26E+10
252.315	1	87	3.76E+09	-1.45	0.17	E	6.35E+09	-1.22	0.05	E	7.57E+09	-1.14	0.03	E	1.90E+09
252.755	2	93	6.23E+09	-1.22	0.02	E	6.27E+09	-1.22	0.01	E	1.90E+09	-1.74	0.06	E	7.30E+09
253.740	3	115	5.64E+06	-4.27	0.00	E	1.40E+06	-4.87	0.41	E	4.36E+07	-3.38	0.71	E	3.00E+08
254.080	1	86	6.36E+08	-2.21	0.00	E	2.45E+08	-2.62	0.21	E	1.57E+08	-2.82	0.29	E	1.30E+09
254.343	2	92	1.15E+09	-1.95	0.00	E	2.20E+09	-1.67	0.07	E	1.68E+09	-1.79	0.15	E	9.00E+08
255.455	1	85	1.32E+09	-1.89	0.02	E	4.00E+09	-1.41	0.04	E	3.19E+09	-1.51	0.07	E	1.20E+09
256.294	2	90	2.45E+10	-0.62	0.24	E	9.13E+09	-1.05	0.10	E	6.50E+10	-0.19	0.11	E	4.06E+10
257.835	1	81	2.48E+09	-1.61	0.02	E	7.62E+09	-1.12	0.05	E	1.64E+10	-0.79	0.06	E	2.40E+09
258.351	1	80	8.72E+09	-1.06	0.02	E	2.37E+09	-1.63	0.15	E	2.33E+09	-1.63	0.19	E	9.40E+09
258.922	1	79	5.26E+10	-0.28	0.45	D	4.51E+10	-0.34	0.04	E	3.73E+10	-0.43	0.04	E	5.09E+10
260.288	1	78	7.26E+09	-1.13	0.08	E	6.94E+09	-1.15	0.10	E	9.60E+07	-3.01	0.13	E	6.60E+09
260.413[k]	1	76	1.85E+09	-1.73	0.01	E	1.56E+10	-0.80	0.06	E	1.47E+10	-0.83	0.05	E	3.30E+09
260.413[k]	2	89	1.33E+10	-0.87	0.03	E	7.03E+07	-3.15	0.33	E	4.19E+09	-1.37	0.01	E	4.16E+10
260.472	1	75	8.05E+09	-1.09	0.01	E	3.59E+08	-2.44	0.14	E	2.66E+08	-2.57	0.19	E	5.90E+09
260.611	2	88	5.20E+10	-0.28	0.51	D	5.02E+10	-0.29	0.05	E	5.23E+10	-0.27	0.05	E	5.22E+10
261.223	2	87	9.95E+10	0.01	0.56	D+	1.07E+11	0.04	0.04	E	9.70E+10	0.00	0.04	E	7.59E+10
261.820	1	74	3.69E+09	-1.42	0.01	E	2.32E+09	-1.62	0.01	E	7.32E+09	-1.12	0.11	E	4.70E+09
263.632	1	73	3.48E+09	-1.44	0.01	E	2.40E+09	-1.60	0.14	E	2.81E+09	-1.53	0.12	E	3.60E+09

(continued on next page)

Table 3 (*continued*)

			HFR[c]				RCI-A[d]				RCI-B[e]				RYA[f]
λ[a] (Å)	i[b]	k[b]	gA (s^{-1})	log gf	CF[g]	Unc.[h]	gA[i] (s^{-1})	log gf[i]	dT[j]	Unc.[h]	gA[i] (s^{-1})	log gf[i]	dT[j]	Unc.[h]	gA (s^{-1})
264.460[k]	1	72	1.51E+11	0.20	0.61	C	1.58E+11	0.22	0.04	E	1.51E+11	0.20	0.02	E	1.50E+11
264.460[k]	3	111	1.01E+11	0.03	0.34	D+	1.16E+11	0.09	0.04	E	9.46E+10	0.00	0.05	E	8.78E+10
264.588	2	85	1.22E+10	-0.89	0.10	E	6.59E+10	-0.16	0.04	E	6.78E+10	-0.15	0.00	E	2.07E+10
265.043	2	84	6.61E+10	-0.16	0.41	D+	7.67E+09	-1.09	0.09	E	4.60E+09	-1.32	0.11	E	6.56E+10
265.286	1	71	2.79E+10	-0.53	0.08	E	1.70E+10	-0.75	0.11	E	1.73E+10	-0.74	0.12	E	2.68E+10
265.755	2	83	1.42E+10	-0.82	0.03	E	1.09E+10	-0.94	0.07	E	1.04E+10	-0.96	0.07	E	1.46E+10
265.976	2	82	2.35E+09	-1.60	0.01	E	1.23E+10	-0.88	0.07	E	5.05E+09	-1.27	0.01	E	3.90E+09
266.344	3	110	3.09E+10	-0.49	0.77	E	2.90E+10	-0.51	0.11	E	3.04E+10	-0.49	0.06	E	3.87E+10
266.513	1	70	1.30E+11	0.14	0.72	C	1.52E+11	0.21	0.04	E	1.37E+11	0.16	0.00	E	1.28E+11
267.144	2	81	1.55E+10	-0.78	0.04	E	7.58E+09	-1.09	0.04	E	4.89E+09	-1.28	0.04	E	1.52E+10
267.292	1	68	6.83E+09	-1.14	0.02	E	1.16E+10	-0.91	0.09	E	1.30E+10	-0.86	0.11	E	7.00E+09
268.052	4	139	8.88E+10	-0.02	0.74	E	2.85E+08	-2.51	0.53	E	2.87E+08	-2.51	0.74	E	1.65E+11
268.309	2	79	4.57E+09	-1.31	0.07	E	2.12E+10	-0.64	0.05	E	1.94E+10	-0.68	0.02	E	3.70E+09
268.721	1	67	6.59E+09	-1.15	0.04	E	1.56E+10	-0.77	0.03	E	1.36E+10	-0.83	0.03	E	7.40E+09
269.011	1	66	1.04E+10	-0.95	0.25	E	1.85E+09	-1.70	0.06	E	4.11E+08	-2.35	0.06	E	1.19E+10
269.257	1	65	1.27E+09	-1.86	0.01	E	1.55E+09	-1.77	0.14	E	1.74E+09	-1.72	0.04	E	2.20E+09
269.777	2	78	2.21E+10	-0.62	0.22	E	4.02E+10	-0.36	0.07	E	5.11E+07	-3.25	0.65	E	1.74E+10
269.815	2	77	9.60E+08	-1.98	0.01	E	9.56E+08	-1.98	0.01	E	1.84E+09	-1.70	0.14	E	1.50E+09
269.903	2	76	4.72E+09	-1.29	0.01	E	1.10E+10	-0.92	0.02	E	7.04E+09	-1.11	0.01	E	6.20E+09
269.969	3	107	6.15E+10	-0.17	0.12	D+	2.76E+10	-0.52	0.11	E	2.74E+10	-0.52	0.06	E	6.86E+10
271.159	4	138	2.63E+11	0.46	0.52	C+	2.95E+11	0.51	0.12	D	3.73E+11	0.61	0.12	D	2.54E+11
271.425	2	74	1.63E+10	-0.75	0.03	E	2.20E+09	-1.61	0.02	E	3.42E+10	-0.42	0.07	E	1.60E+10
272.257	4	136	6.73E+06	-4.13	0.01	E	7.52E+08	-2.08	0.05	E	4.35E+08	-2.32	0.00	E	5.00E+08
273.369	2	73	3.44E+09	-1.42	0.01	E	2.13E+09	-1.62	0.09	E	2.20E+09	-1.61	0.10	E	3.30E+09
273.988	1	64	1.25E+10	-0.85	0.03	E	8.73E+09	-1.01	0.17	E	8.42E+09	-1.02	0.18	E	1.15E+10
275.402	3	106	1.68E+10	-0.72	0.49	E	4.31E+09	-1.31	0.02	E	1.96E+09	-1.65	0.02	E	2.02E+10
276.475	2	70	1.78E+09	-1.69	0.05	E	2.23E+09	-1.59	0.06	E	1.97E+09	-1.65	0.04	E	5.82E+09
277.205	2	69	1.73E+10	-0.70	0.10	E	1.54E+10	-0.75	0.17	E	1.49E+10	-0.77	0.19	E	1.75E+10
278.857	2	67	3.62E+09	-1.38	0.01	E	4.28E+09	-1.30	0.12	E	3.98E+09	-1.33	0.05	E	3.90E+09
279.434	2	65	6.28E+08	-2.13	0.01	E	7.22E+08	-2.07	0.02	E	3.49E+08	-2.39	0.13	E	7.00E+08
285.131[k]	1	62	2.51E+10	-0.51	0.13	E	2.16E+10	-0.58	0.13	E	2.11E+10	-0.59	0.15	E	2.49E+10
285.131[k]	4	131	2.26E+11	0.44	0.35	C+	4.34E+10	-0.28	0.12	E	1.15E+11	0.15	0.08	E	2.41E+11
288.297	4	130	2.19E+10	-0.57	0.05	E	6.11E+08	-2.12	0.32	E	1.41E+10	-0.76	0.01	E	1.45E+10
293.396	1	60	3.30E+11	0.63	0.71	C+	1.96E+11	0.40	0.10	E	2.13E+11	0.44	0.13	D	3.28E+11
293.717	2	63	2.46E+11	0.50	0.71	C+	1.41E+11	0.26	0.11	E	1.51E+11	0.29	0.14	E	2.42E+11
295.494	1	59	1.15E+11	0.18	0.33	E	1.26E+11	0.22	0.10	E	9.16E+10	0.08	0.11	E	1.78E+11
295.968	1	58	3.46E+11	0.66	0.87	C+	2.17E+11	0.45	0.08	E	2.26E+11	0.47	0.10	E	3.50E+11
296.556	2	62	2.92E+11	0.59	0.53	C+	1.73E+11	0.36	0.08	E	1.84E+11	0.39	0.10	E	2.91E+11
297.186	3	98	1.88E+11	0.40	0.81	C+	1.31E+11	0.24	0.12	E	1.23E+11	0.21	0.08	E	2.06E+11
297.878	2	61	1.15E+11	0.18	0.81	C	6.94E+10	-0.03	0.12	E	7.95E+10	0.02	0.14	E	1.36E+11
298.768	3	97	1.03E+11	0.14	0.47	C	6.69E+10	-0.05	0.12	E	6.73E+10	-0.05	0.10	E	1.03E+11
300.518	1	57	4.26E+10	-0.24	0.12	E	2.23E+10	-0.52	0.10	E	2.36E+10	-0.50	0.10	E	6.27E+09
305.506	2	60	1.71E+10	-0.62	0.07	E	1.71E+10	-0.62	0.07	E	1.63E+10	-0.64	0.09	E	1.76E+10
307.790	2	59	1.21E+08	-2.76	0.00	E	4.53E+07	-3.19	0.39	E	1.43E+08	-2.69	0.08	E	2.00E+08
309.036	3	96	1.30E+09	-1.73	0.09	E	4.61E+08	-2.18	0.18	E	1.24E+09	-1.75	0.14	E	2.20E+09
310.789	1	53	3.73E+09	-1.27	0.01	E	1.97E+09	-1.55	0.11	E	1.71E+09	-1.61	0.13	E	3.80E+09
312.997	1	52	5.11E+09	-1.12	0.06	E	3.68E+09	-1.27	0.06	E	7.08E+09	-0.98	0.07	E	9.20E+09
316.757	1	51	1.64E+09	-1.61	0.00	E	1.29E+09	-1.71	0.14	E	2.63E+08	-2.40	0.07	E	2.20E+09
321.995	1	50	3.65E+09	-1.25	0.05	E	2.65E+09	-1.38	0.09	E	2.67E+09	-1.38	0.13	E	3.50E+09
322.683	2	54	4.01E+09	-1.21	0.01	E	2.68E+09	-1.38	0.11	E	2.59E+09	-1.39	0.13	E	3.40E+09
324.420	2	53	6.71E+07	-2.98	0.00	E	1.55E+08	-2.61	0.13	E	1.98E+08	-2.50	0.16	E	1.00E+08
325.014	1	49	1.48E+09	-1.63	0.00	E	5.06E+07	-3.10	0.13	E	1.32E+09	-1.68	0.06	E	1.80E+09
330.920	2	51	1.09E+09	-1.74	0.02	E	9.90E+08	-1.79	0.10	E	6.04E+08	-2.00	0.19	E	9.00E+08
334.389	1	48	1.13E+09	-1.72	0.00	E	3.35E+08	-2.25	0.05	E	3.51E+08	-2.23	0.16	E	1.00E+09
336.636	2	50	1.24E+08	-2.68	0.00	E	4.24E+08	-2.14	0.07	E	4.09E+08	-2.16	0.07	E	2.00E+08
339.937	2	49	1.69E+08	-2.54	0.00	E	1.63E+08	-2.55	0.06	E	2.97E+08	-2.29	0.28	E	2.00E+08
358.746	1	45	7.13E+08	-1.86	0.01	E	1.29E+08	-2.60	0.28	E	3.32E+08	-2.19	0.10	E	1.00E+08
366.035	1	42	1.44E+09	-1.54	0.02	E	2.65E+08	-2.27	0.22	E	4.97E+08	-2.00	0.01	E	3.00E+08
371.215	1	39	1.04E+09	-1.67	0.03	E	3.77E+08	-2.11	0.25	E	5.13E+08	-1.97	0.01	E	3.10E+08
371.251	2	47	1.99E+09	-1.39	0.05	E	4.14E+08	-2.07	0.20	E	9.45E+08	-1.71	0.03	E	5.70E+08
374.829	2	46	1.33E+09	-1.55	0.05	E	3.68E+08	-2.11	0.17	E	2.91E+08	-2.21	0.11	E	4.40E+08
375.116	1	38	6.31E+09	-0.88	0.04	E	2.66E+09	-1.25	0.13	E	3.27E+09	-1.16	0.30	E	2.11E+09
377.017	2	45	1.48E+08	-2.50	0.01	E	1.76E+07	-3.43	0.14	E	8.42E+07	-2.75	0.31	E	2.00E+07
378.926	1	37	1.70E+09	-1.44	0.04	E	7.07E+08	-1.82	0.04	E	8.74E+08	-1.73	0.21	E	6.40E+08
381.565	1	34	3.12E+09	-1.17	0.05	E	9.34E+08	-1.69	0.16	E	1.11E+09	-1.62	0.34	E	1.22E+09
382.644	2	44	9.55E+08	-1.68	0.07	E	2.69E+07	-3.23	0.25	E	8.17E+07	-2.75	0.29	E	4.30E+08
384.088	2	43	1.61E+08	-2.45	0.02	E	3.78E+06	-4.08	0.11	E	1.48E+07	-3.48	0.23	E	5.00E+07
384.473	1	33	7.63E+08	-1.77	0.02	E	1.65E+08	-2.44	0.11	E	3.22E+08	-2.15	0.30	E	2.90E+08
385.080	2	42	2.98E+09	-1.18	0.09	E	1.27E+09	-1.55	0.11	E	1.62E+09	-1.44	0.25	E	1.37E+09
385.146	2	41	9.80E+09	-0.66	0.05	E	1.84E+09	-1.39	0.10	E	4.58E+09	-0.99	0.29	E	3.85E+09
385.906	1	32	1.02E+09	-1.64	0.02	E	7.70E+07	-2.76	0.12	E	1.14E+08	-2.60	0.15	E	3.40E+08
387.043	2	40	1.41E+09	-1.50	0.05	E	4.72E+08	-1.97	0.08	E	5.44E+08	-1.91	0.16	E	5.00E+08

(*continued on next page*)

Table 3 (*continued*)

			HFR[c]				RCI-A[d]				RCI-B[e]				RYA[f]
λ[a] (Å)	*i*[b]	*k*[b]	*gA* (s^{-1})	*log gf*	*CF*[g]	*Unc.*[h]	*gA*[i] (s^{-1})	*log gf*[i]	*dT*[j]	*Unc.*[h]	*gA*[i] (s^{-1})	*log gf*[i]	*dT*[j]	*Unc.*[h]	*gA* (s^{-1})
389.138	1	30	2.57E+09	-1.23	0.04	E	2.03E+09	-1.34	0.17	E	2.65E+09	-1.22	0.32	E	1.19E+09
390.818	2	39	5.38E+08	-1.91	0.03	E	2.62E+08	-2.22	0.01	E	1.63E+08	-2.43	0.14	E	4.00E+08
392.069	1	29	8.85E+08	-1.69	0.08	E	2.56E+08	-2.23	0.08	E	2.68E+08	-2.21	0.32	E	3.60E+08
392.664	1	28	3.97E+09	-1.04	0.06	E	1.84E+09	-1.37	0.09	E	1.79E+09	-1.38	0.14	E	1.63E+09
395.047	1	26	2.08E+09	-1.31	0.06	E	1.24E+09	-1.54	0.12	E	2.08E+09	-1.31	0.29	E	1.34E+09
396.621	1	25	1.68E+08	-2.40	0.02	E	9.30E+07	-2.66	0.04	E	9.94E+07	-2.63	0.24	E	1.10E+08
396.865	1	24	6.31E+09	-0.83	0.11	E	3.50E+09	-1.08	0.14	E	3.02E+09	-1.15	0.31	E	2.51E+09
399.128	1	23	6.64E+09	-0.80	0.11	E	2.07E+09	-1.31	0.13	E	1.51E+09	-1.44	0.31	E	3.01E+09
399.377	2	37	1.19E+10	-0.55	0.09	E	5.22E+09	-0.90	0.15	E	5.56E+09	-0.88	0.32	E	5.35E+09
400.446	1	22	6.73E+08	-1.79	0.10	E	4.61E+08	-1.96	0.13	E	4.31E+08	-1.98	0.34	E	2.70E+08
400.485	2	36	4.06E+08	-2.01	0.03	E	8.28E+07	-2.70	0.16	E	1.11E+08	-2.57	0.31	E	1.70E+08
401.260	2	35	1.75E+09	-1.37	0.04	E	1.42E+08	-2.47	0.08	E	3.97E+08	-2.02	0.21	E	5.60E+08
403.544	1	20	4.35E+08	-1.97	0.04	E	1.91E+08	-2.33	0.05	E	2.32E+08	-2.25	0.24	E	1.20E+08
403.625	1	19	4.52E+09	-0.96	0.08	E	1.87E+09	-1.34	0.19	E	1.67E+09	-1.39	0.36	E	2.15E+09
405.868	1	18	1.32E+09	-1.49	0.04	E	3.26E+08	-2.09	0.07	E	2.95E+08	-2.14	0.30	E	5.10E+08
408.576	1	17	2.25E+08	-2.25	0.01	E	8.58E+06	-3.67	0.11	E	2.01E+07	-3.30	0.36	E	1.00E+08
410.354	2	31	2.22E+09	-1.25	0.07	E	6.30E+08	-1.80	0.20	E	5.59E+08	-1.85	0.38	E	3.60E+08
410.589	1	16	3.03E+08	-2.12	0.01	E	2.37E+07	-3.22	0.13	E	3.46E+07	-3.06	0.04	E	2.00E+08
410.739[k]	1	15	4.57E+08	-1.94	0.03	E	2.26E+08	-2.24	0.03	E	2.39E+08	-2.22	0.21	E	2.70E+08
410.739[k]	2	30	3.97E+09	-1.00	0.06	E	1.68E+09	-1.37	0.14	E	1.55E+09	-1.41	0.35	E	1.69E+09
412.636	1	13	2.52E+09	-1.19	0.08	E	1.31E+09	-1.48	0.11	E	1.22E+09	-1.51	0.34	E	9.70E+08
416.227	1	12	4.52E+08	-1.93	0.03	E	1.09E+08	-2.55	0.19	E	9.81E+07	-2.59	0.37	E	1.30E+08
416.639	2	27	3.26E+08	-2.07	0.03	E	4.64E+06	-3.92	0.05	E	5.75E+06	-3.83	0.23	E	1.40E+08
419.820	1	11	4.21E+09	-0.95	0.07	E	2.06E+09	-1.26	0.12	E	1.89E+09	-1.30	0.35	E	1.89E+09
420.089	1	10	1.19E+09	-1.50	0.08	E	8.00E+08	-1.67	0.08	E	6.00E+08	-1.80	0.30	E	5.80E+08
421.885	2	23	7.39E+08	-1.71	0.02	E	4.51E+08	-1.92	0.12	E	4.15E+08	-1.96	0.36	E	3.90E+08
425.728	2	21	2.55E+08	-2.16	0.03	E	3.78E+04	-5.99	0.99	E	1.47E+05	-5.40	0.96	E	1.00E+08
426.460	1	9	2.08E+09	-1.25	0.03	E	1.04E+09	-1.55	0.20	E	9.92E+08	-1.57	0.40	E	1.00E+09
426.819	2	20	7.91E+08	-1.67	0.06	E	3.17E+08	-2.06	0.15	E	2.49E+08	-2.17	0.36	E	3.70E+08
429.417	2	18	3.81E+07	-2.98	0.00	E	1.29E+08	-2.45	0.04	E	1.50E+08	-2.38	0.26	E	3.00E+07
431.631	1	8	8.73E+08	-1.62	0.07	E	3.19E+08	-2.05	0.06	E	2.44E+08	-2.17	0.34	E	4.00E+08
432.452	2	17	1.81E+08	-2.30	0.01	E	1.18E+08	-2.48	0.11	E	1.05E+08	-2.53	0.35	E	9.00E+07
433.282	1	7	8.08E+07	-2.64	0.01	E	4.96E+07	-2.86	0.15	E	2.52E+07	-3.15	0.03	E	6.00E+07
434.872	2	15	6.25E+08	-1.75	0.02	E	3.26E+08	-2.03	0.18	E	3.03E+08	-2.07	0.39	E	3.20E+08
435.920	2	14	3.23E+08	-2.04	0.03	E	7.33E+07	-2.68	0.05	E	6.97E+07	-2.70	0.31	E	1.40E+08
436.555	1	6	4.08E+08	-1.94	0.04	E	4.08E+08	-1.93	0.08	E	3.79E+08	-1.97	0.34	E	2.30E+08
441.032	2	12	2.68E+08	-2.11	0.05	E	2.02E+08	-2.23	0.08	E	1.78E+08	-2.28	0.35	E	1.20E+08
445.324	1	5	2.23E+08	-2.18	0.01	E	1.56E+08	-2.33	0.13	E	1.27E+08	-2.42	0.38	E	1.20E+08
445.373	2	10	1.96E+08	-2.24	0.01	E	1.41E+08	-2.38	0.05	E	1.23E+08	-2.44	0.30	E	1.00E+08
452.543	2	9	1.51E+08	-2.33	0.02	E	9.60E+07	-2.53	0.09	E	9.02E+07	-2.56	0.36	E	8.00E+07
473.842	2	5	4.45E+07	-2.83	0.01	E	2.53E+07	-3.07	0.02	E	2.03E+07	-3.17	0.29	E	2.00E+07

[a] Experimental values from Ryabtsev et al. [5];
[b] Lower and upper level indices, respectively *i* and *k*, given in the first column of Table 2.
[c] Our HFR calculation;
[d] Our MCDHF-RCI-A calculation;
[e] Our MCDHF-RCI-B calculation;
[f] Hartree–Fock calculation of Ryabtsev et al. [5];
[g] Cancellation factor as defined in Cowan [7];
[h] Uncertainty indicator as defined by NIST [11], here C+ ≤ 18%, C ≤ 25%, D+ ≤ 40%, D ≤ 50%, E > 50%, evaluated with respect to the *gA*-values of Ryabtsev et al. [5] using the methodology described by Kramida [12];
[i] Given in the Babushkin gauge;
[j] Uncertainty indicator as defined in Ekman et al. [10];
[k] Doubly classified in Ryabtsev et al. [5].

ence values to deduce the uncertainty indicator (*Unc.* columns in Table 3) as defined by NIST [11] following the procedure described by Kramida [12]. From that table, one notices that two relatively strong transitions predicted by Ryabtsev et al. [5], *i.e.* lines at 223.172 Å with $gA_{RYA} = 6.13E + 10$ s^{-1} and at 231.451 Å with $gA_{RYA} = 4.91E + 10$ s^{-1}, are affected by strong cancellation effects in our HFR model with CF of, respectively, 0.05 and 0.03, and corresponding gA_{HFR}-values of 5.13E+08 and 1.59E+07 s^{-1}. In Fig. 4, a comparison of our HFR transition probabilities, gA_{HFR}, with respect to the calculation of Ryabtsev et al. [5], gA_{RYA}, is shown. The ratio, gA_{HFR}/gA_{RYA}, is plotted versus our HFR line strength, S_{HFR}, both in logarithmic scale. Similar plots are displayed for our MCDHF-RCI-A model in Fig. 5 and for our MCDHF-RCI-B model in Fig. 6. In these three figures, one can see that a large scatter of up to several orders of magnitudes occurs for the weak transitions, *i.e.* having a small line strength (typically $S < 1$ a.u.). Most of these discrepancies can be explained by the fact that the majority of these transitions are affected by strong cancellation effects (with $CF < 0.05$) that render weak lines even weaker [7] or by a strong gauge disagreement (with $dT > 0.1$). They both indicate a strong model sensitivity.

Concerning the strongest transitions(with $S \geq 1$ a.u.), the average ratio of our transition probabilities with respect to the values calculated by Ryabtsev et al. [5], used as reference, is equal to 0.97 with a standard deviation of 0.08 for our HFR model, to 0.93 with a standard deviation of 0.41 for our MCDHF-RCI-A model, and to 0.81 with a standard deviation of 0.26 for our MCDHF-RCI-B model. First, it denotes a better agreement (by a few percent) between both HFR models. Second, although both our MCDHF models produce systematically lower rates (by ∼10 % for MCDHF-RCI-A and

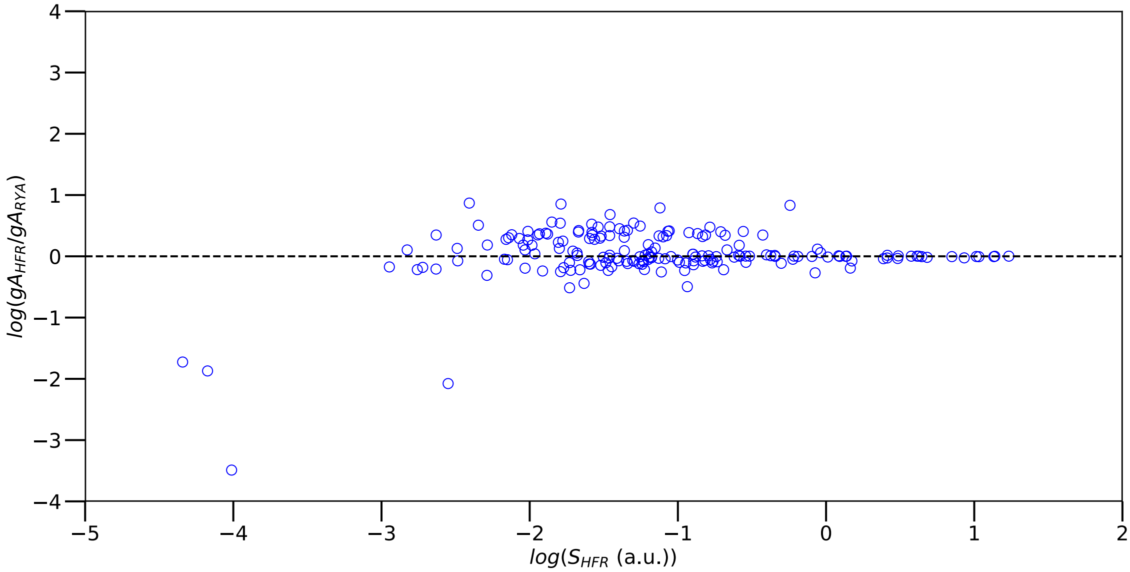

Fig. 4. Comparison of our HFR transition probabilities, gA_{HFR}, with respect to the values calculated by Ryabtsev et al. [5], gA_{RYA}. The ratio, gA_{HFR}/gA_{RYA}, is plotted versus our HFR line strength, S_{HFR}, both in logarithmic scale. Black dashed line: straight line of equality. The average and the standard deviation of the ratios is respectively equal to 0.97 and 0.08 for a sample restricted to the strongest lines, *i.e.* $S_{HFR} \geq 1$ a.u. This plot is used to evaluate the uncertainty indicator as defined in NIST [11] on our HFR rates following the procedure described by Kramida [12].

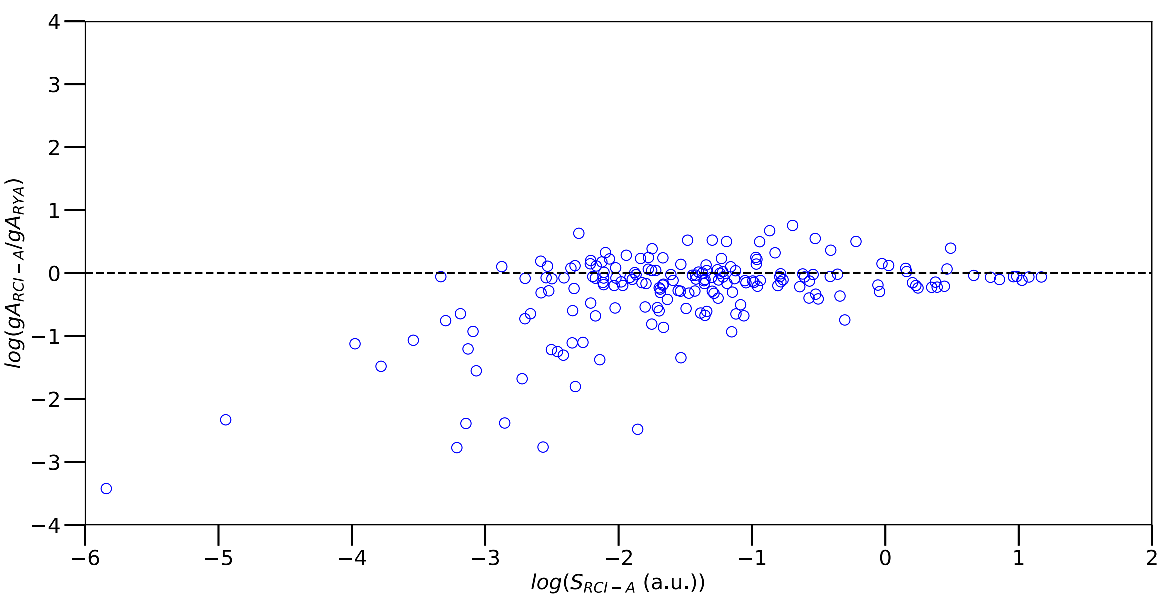

Fig. 5. Comparison of our MCDHF-RCI-A transition probabilities corrected with the experimental wavelengths [5], gA_{RCI-A}, with respect to the values calculated by Ryabtsev et al. [5], gA_{RYA}. The ratio, gA_{RCI-A}/gA_{RYA}, is plotted versus our RCI-A line strength, S_{RCI-A}, both in logarithmic scale. Black dashed line: straight line of equality. The average and the standard deviation of the ratios is respectively equal to 0.93 and 0.41 for a sample restricted to the strongest lines, *i.e.* $S_{RCI-A} \geq 1$ a.u. This plot is used to evaluate the uncertainty indicator as defined in NIST [11] on our MCDHF-RCI-A rates following the procedure described by Kramida [12].

by ∼20 % for MCDHF-RCI-B) than in both HFR models, the strategy adopted in our MCDHF-RCI-B model improves the accord with the latter as the standard deviation of the ratios has reduced by a half.

4. Conclusions

The Hf VI radiative parameters have been calculated for the 185 E1 transitions observed by Ryabtsev et al. [5] in the UV range from 193 Å to 474 Å. As no experimental determination of radiative rates is available in the literature, a multiplaform approach has been adopted to carry out the present calculations so as to estimate the accuracy of the computed rates. From the comparisons of our three independent models based on both the HFR [7] and MCDHF [8,9] methods along with the calculations published by Ryabtsev et al. [5] that they used for line classification purpose, it was found that the uncertainties affecting the theoretical rates range from a few percent (for our HFR model) to ∼40 % (for our MCDHF-RCI-A model) for the strong E1 transitions with $S \geq 1$ a.u. With respect to the other lines, they can be highly inaccurate with uncertainties far more than 100 % due to strong cancellation effects and important gauge disagreements that render the rates highly model sensitive. This is essentially caused by the strong mixing affecting most of

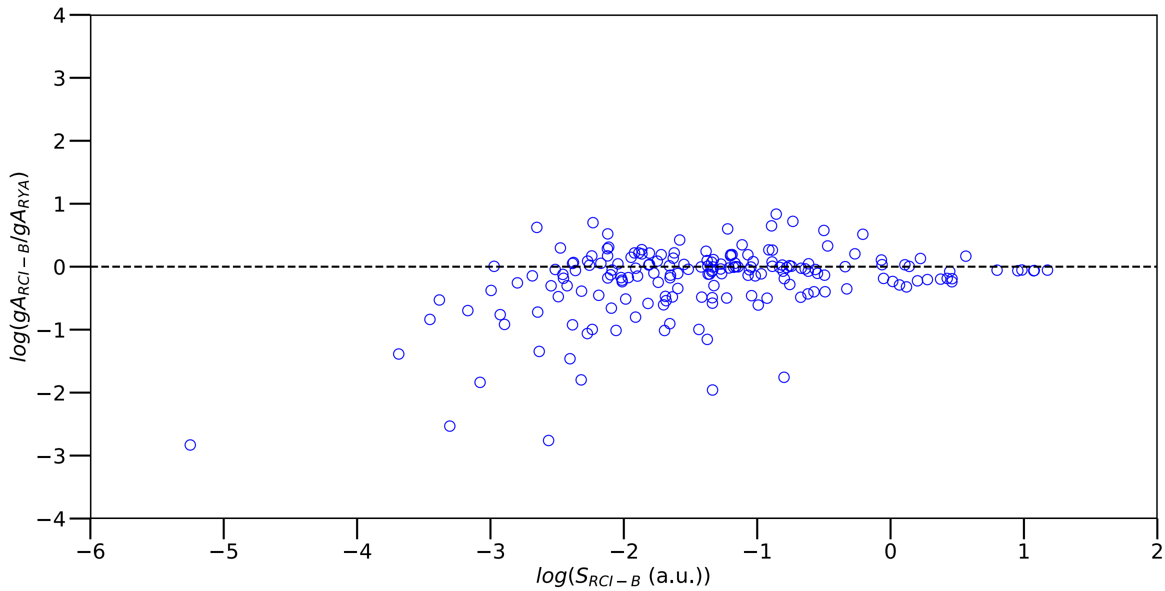

Fig. 6. Comparison of our MCDHF-RCI-B transition probabilities corrected with the experimental wavelengths [5], gA_{RCI-B}, with respect to the values calculated by Ryabtsev et al. [5], gA_{RYA}. The ratio, gA_{RCI-B}/gA_{RYA}, is plotted versus our RCI-B line strength, S_{RCI-B}, both in logarithmic scale. Black dashed line: straight line of equality. The average and the standard deviation of the ratios is respectively equal to 0.81 and 0.26 for a sample restricted to the strongest lines, *i.e.* $S_{RCI-B} \geq 1$ a.u. This plot is used to evaluate the uncertainty indicator as defined in NIST [11] on our MCDHF-RCI-B rates following the procedure described by Kramida [12].

the Hf VI atomic states. Finally, we recommend our HFR rates except for the two lines at 223.172 Å and at 231.451 Å where the *gA*-values of Ryabtsev et al. [5] should be used instead with an uncertainty indicator *Unc.* equal to E (> 50 %), due to strong cancellation effects affecting the former for these two transitions.

Declaration of Competing Interest

The authors declare that they have no known competing financial interests or personal relationships that could have appeared to influence the work reported in this paper.

Data availability

Data will be made available on request.

Acknowledgments

PQ and PP are respectively Research Director and Research Associate of the Belgian Fund for Scientific Research F.R.S.-FNRS. Financial support from this organization is gratefully acknowledged. EBM is grateful to Belgian colleagues for their hospitality during his stay at Université de Mons - UMONS. EBM and SEY were supported by Marien Ngouabi University from Congo.

References

[1] Linsmeier C, Rieth M, Aktaa J, Chikada T, Hoffmann A, Houden A, Kurishita H, Jin X, Li M, Litnovsky A, Matsuo S, von Müller A, Nikolic V, Palacios T, Rippan R, Qu S, Reiser J, Riesch J, Shikama T, Stieglitz R, Weber T, Wurster S, J-H Y, Zhou Z. Development of advanced high heat flux and plasma-facing materials. Nucl Fusion 2017;57:092007. doi:10.1088/1741-4326/aa6f71.

[2] Pillon M, Angelone M, Forrest RA. Measurements of fusion-induced decay heat in materials and comparison with code predictions. Radiat Phys Chem 2004;71:895. doi:10.1016/j.radphyschem.2004.04.119.

[3] Gilbert MR, J-C S. Neutron-induced transmutation effects in W and W-alloys in a fusion environment. Nucl Fusion 2011;51:043005. doi:10.1088/0029-5515/51/4/043005.

[4] Ryabtsev AN, Ya KE, Kildiyarova RR, Tchang-Brillet W-Ü L, J-F W. $4f^{13}5s^25p^6$ – $4f^{13}5s^25p^56s$ transitions in the W VIII spectrum and spectra of isoelectronic hafnium, tantalum, and rhenium ions. Opt Spectrosc 2012;113:109. doi:10.1134/S0030400X12080140.

[5] Ryabtsev AN, Ya KE, Kildiyarova RR, Tchang-Brillet W-Ü L, J-F W, Champion N, Blaess C. Spectra of the W VIII isoelectronic sequence: I. hf VI. Phys Scr 2014;89:115402. doi:10.1088/0031-8949/89/11/115402.

[6] Bokamba Motoumba E, Enzonga Yoca S, Quinet P, Palmeri P. Calculations of transition rates in erbium-like ions Lu IV, Hf v and Ta VI using the ab initio MCDHF-RCI and semi-empirical HFR methods. ADNDT 2020;133-134:101340.

[7] Cowan RD. The theory of atomic structure and spectra. Berkeley: University of California Press; 1981.

[8] Froese Fischer C, Gaigalas G, Jönsson P, Bieroń J, Grant IP. GRASP2018-a fortran 95 version of the general relativistic atomic structure package. Comput Phys Commun 2019;237:184.

[9] Grant IP. Relativistic quantum theory of atoms and molecules. Theory and computation. New York: Springer; 2007.

[10] Ekman J, Godefroid M, Hartman H. Validation and implementation of uncertainty estimates of calculated transition rates. Atoms 2014;2:215.

[11] Kramida A., Yu R., Reader J., NIST ASD Team. NIST atomic spectra database (ver. 5.10). 2022. [Online]. Available: https://physics.nist.gov/asd [2023, January 18]. National Institute of Standards and Technology, Gaithersburg, 10.18434/T4W30F.

[12] Kramida A. Critical evaluation of data on atomic energy levels, wavelengths, and transition probabilities. Fusion Sci. Technol. 2013;63:313.